Biogeosciences Discuss., 7, 7849–7902, 2010
www.biogeosciences-discuss.net/7/7849/2010/
doi:10.5194/bgd-7-7849-2010

Biogeosciences Discussions

Influence of distributary channels on sediment and organic carbon supply in event-dominated coastal margins: the Po prodelta as a study case

T. Tesi[1,2], S. Miserocchi[1], M. A. Goñi[2], M. Turchetto[3], L. Langone[1], A. De Lazzari[3], S. Albertazzi[1], and A. Correggiari[1]

[1]Istituto Scienze Marine CNR – Sede di Bologna, Via P. Gobetti 101, 40129 Bologna, Italy
[2]College of Oceanic and Atmospheric Science, Oregon State University, Corvallis, OR 97331, USA
[3]Istituto Scienze Marine CNR – Sede di Venezia, Castello 1364/A, 30122 Venice, Italy

Received: 28 September 2010 – Accepted: 21 October 2010 – Published: 28 October 2010

Correspondence to: T. Tesi (tommaso.tesi@bo.ismar.cnr.it)

Published by Copernicus Publications on behalf of the European Geosciences Union.

Abstract

From November 2008 through May 2009, the North Italy experienced the highest precipitation period recorded over the last century. As a result, a long series of flood events occurred in the Po river (North Italy). This series of events ended with a large flood in early May 2009. An event-response sampling was carried out in the Po prodelta in April–May 2009 to characterize this latter event and to investigate the strata preservation in the stratigraphy record as a result of this series of floods. The water sampling was carried out during two periods of the flood, including early in the event under conditions of moderate river flow (~5000 $m^3 s^{-1}$) and 24 h later during the peak discharge (~8000 $m^3 s^{-1}$). At each station, profiles of conductivity, transmittance, and fluorescence were acquired whereas surface and bottom waters were sampled to collect sediments in suspension. In addition, sediment cores were collected in the Po prodelta before and after the peak flood. Biogeochemical compositions and sedimentological characteristics of suspended and sediment samples were investigated using a multi-proxy approach that included bulk and biomarkers analyses. Furthermore, ^{7}Be down-core profiles and radiographs were used to analyze the internal stratigraphy of sediment cores.

During moderate discharge, the water column did not show evidence of plume penetration. In surface waters, suspended sediment concentrations were found to be similar to low river discharge periods whereas the main OC was autochthonous. After 24 h, during the peak flood, water column properties and biogeochemical parameters exhibited marked changes indicating significant penetration of the turbid plume. However, suspended sediment concentrations and terrigenous OC content in surface waters were still less then expected based on the discharge. These results suggested that, since material enters the Adriatic as buoyancy-driven flow with a reduced transport capacity, settling and flocculation processes result in trapping a significant fraction of land-derived material prior to reaching the subaqueous prodelta.

BGD
7, 7849–7902, 2010

In spite numerous floods occurred from November 2008 through April 2009, sediment cores collected in late April 2009 did not exhibited significant evidence of event-strata preservation. Since these floods were ordinary (2–3 y return period), the lack of preservation indicates that most of the sediment supply during these oridinary events does not reach the subaqueous prodelta. However, it is likely that modest sediment deposition occurs during these oridinary floods but thicknesses of these event-strata are not sufficient to compete with post-depositional processes.

Stations in the north and central prodelta were re-occupied after the peak of the May 2009 flood. Based on ^{7}Be and radiographs, we estimated that 17 and 6 cm event-layers, respectively. Selective trapping of coarse material occurred in the central prodelta likely because of the geomorphologic setting of the central outlet characterized by an estuary-like mouth. Despite these settling processes, lignin-based parameters indicated that sources of the terrigenous OC were fairly homogenous throughout the channel network and between size-fractions.

1 Introduction

Prodeltas are globally distributed sedimentary architectures located along the modern coastline. Although they gradually formed 6 kyr ago after sea level stabilized, they have recently experienced significant changes in morphology because of human land use changes within watersheds (e.g., deforestation, damming, irrigation, etc.) that have reduced or enhanced sediment supply to the ocean (Syvitski et al., 2005a, b, 2009; Kettner and Syvitski, 2009). However, despite these anthropogenic modifications, deltas are still considered important long-term sinks of reduced carbon accounting for nearly half of the OC burial in marine sediments (Berner, 1987, 1989; Hedges and Keil, 1995). Therefore, even though prodeltas cover a small fraction of the oceanic seafloor, the OC sequestration in these systems contributes to the regulation of atmospheric CO_2 concentrations on geologic time scale and might potentially store anthropogenically-derived CO_2 in the form of reduced modern carbon (Blair et al., 2003; Goni et al., 2005).

BGD
7, 7849–7902, 2010

In this study we focused on the Po prodelta located in the North Adriatic Sea (Mediterranean Sea). In this system, the supply and accumulation of OC are highly episodic because of flood events that ensure a rapid supply and deposition of land-derived OC in the coastal ocean (Palinkas et al., 2005; Wheatcroft et al., 2006; Miserocchi et al., 2007; Tesi et al., 2008). Recently, event-dominated rivers like the Po have received renewed consideration as they account for ~50% of the sediment supply to the ocean (Milliman and Syvitski, 1992). Therefore, it has been suggested in several studies that about half of the land-ocean exchange of particulate OC is driven by these event-dominated systems (Gomez et al., 2003; Leithold et al., 2006). As it is not feasible to individually study each watershed, several land-ocean studies have provided general conceptual models to discriminate the major geological and hydrological variables affecting the character of OC supplied to the ocean. For small mountainous rivers, Leithold et al. (2006) suggested that high sediment yields coupled with low weathering history enhances the preservation of the original upland-generated organic carbon signal because the bedrock material is constantly delivered from hillslopes to river channels. In parallel, Wheatcroft et al. (2010) indicated that river discharge exerts first-order control on the concentration and character of OC in event-dominated watersheds. According to the authors, mobilization of distinct pools of OC occurs at different flows and the transport effectiveness of each pool is the product of flow frequency and transport magnitude (i.e., effective discharge).

In this manuscript, we propose the internal architecture of prodeltaic systems as an additional variable affecting the land-ocean exchange of particulate OC because it has been shown that their morphology influences the transfer of sediment to the coastal ocean. A global analysis of world deltas have been carried out by Syvitski et al. (2005b). The authors showed how deltas with a high number of distributary channels produce hypopycnal plumes that reduce transport capacity. Under these conditions, sediments diffuse from the deltaic coastal zone as a buoyancy-driven plume, rather than as a momentum driven-flow. Because of the reduced plume penetration, river material has a high probability to flocculate and settle in shallow waters.

BGD
7, 7849–7902, 2010

In addition, trapping of river-born material can occur within each distributary channel. This storage varies among channels because the response to the upstream discharge is generally not identical for each branch (Syvitski et al., 2005a; Syvitski and Kettner, 2007). As a result, the sediment and OC delivery to the ocean from each mouth is highly irregular throughout time and might not be coherent with the material supplied from the rest of the channel network.

Although a multi-channels setting is a common feature of numerous prodeltas (Syvitski et al., 2005a), there is a lack of general understanding about the influence of prodeltaic architecture on supply and accumulations of OC in the ocean. In order to understand the land-ocean exchange of particulate material in a multi-branch setting, an event-response sampling was carried out in the Northern Adriatic Sea (Mediterranean Sea) when the Po river experienced a significant flood event in May 2009. The Po river consists of 5 major distributaries formed as result of human modifications and natural adjustments. The May 2009 event had a 20-year return period and it was the last in a series of frequent flood events corresponding to the highest precipitation period recorded over the last century (Nanni et al., 2009). Suspended sediments supplied to the prodelta were collected during two periods of the May 2009 flood, including early in the event under conditions of moderate river flow (~5000 $m^3 s^{-1}$) and later during peak discharge (~8000 $m^3 s^{-1}$). In addition, sediment cores were collected after and before the peak discharge. Samples were analyzed using a multi-proxy approach that included determination of suspended sediment concentration (SSC), organic carbon (OC), total nitrogen (TN), alkaline CuO reaction products, carbon isotope compositions ($\delta^{13}C$ and $\Delta^{14}C$), grain-size, and mineral surface area (SA). In addition, ^{7}Be down-core profiles and radiographs, were used to estimate thickness and investigate the internal stratigraphy of the flood deposit.

The main goal of this time-series analysis was to asses the role of distributary channels in affecting the land-ocean exchange of particulate OC and characterize the non-steady-state OC deposition in event-dominated coastal margins and. First, we will provide background information about the Po river and prodelta that have been heavily

BGD
7, 7849–7902, 2010

studied since October 2000, when the Po river experienced a large flood event (i.e., EuroStrataform project). Then, we will focus on the short term variability of the suspended material collected in the prodelta during the May 2009 flood. Finally, sediment cores will be used to understand the timing of sediment accumulation and factors driving the emplacement of particulate OC in the prodelta during flood events.

2 Background

2.1 Po river and delta

With over three millennia of human activity, the 75 000 km^2 Po watershed is one of the most agriculturally developed and populated areas in Europe. Over a third of the drainage basin is mountainous whereas the rest is composed of a wide, low-gradient alluvial plain (Fig. 1a). His basin represents the confluence of Alpine (maximal relief ~4500 m) and Apennine (maximal relief ~2000 m) streams. The river typically experiences two peak discharges, first in autumn because of the rainfall and later in spring mainly driven by snowmelt. Although these seasonal peaks, a third of the total flow is regulated by reservoirs management for hydropower and irrigation purposes. The Po river has a mean freshwater discharge of 1525 m^3 s^{-1} (Boldrin et al., 2005) recorded at Pontalagoscuro gauging station (Fig. 1). Downstream Pontelagoscuro, the river splits in 5 major distributaries (Fig. 1b): Maistra, Pila, Tolle, Gnocca, and Goro, from north to south, respectively (Fig. 1b, c). The main distributary channel is Pila, delivering 74% of the sediment load whereas Maistra, Tolle, Gnocca, and Goro supply the remaining 1%, 7%, 10%, and 8%, respectively. Fluxes through distributary channels is variables with time fluctuating between periods of accumulation and net erosion. During moderate river discharge, Pila supplies 61% of the fresh water entering the delta while Maistra, Tolle, Gnocca, and Goro supply the remaining 3%, 12%, 16% and 8%, respectively (Syvitski et al., 2005a). The input of fresh water significantly changes when the river experiences large floods. For example, in the October 2000, during a significant flood

BGD
7, 7849–7902, 2010

event, the Pila fresh water input dropped to 40% while Maistra, Tolle, Gnocca, and Goro distributaries considerably increased their relative supply accounting for 8, 12, 20, and 20% of the total fresh water entering the delta, respectively.

The sediment deposition in the subaqueous prodelta occurs as result of episodic events (i.e. event-driven floods). Recently the river has experienced several major floods, defined as events with mean water discharge rates exceeding 7000 $m^3 s^{-1}$. The most recent events occurred in November 1994, October 2000, and November 2002. The October 2000 flood was particularly significant as the river flow exceeded 9650 $m^3 s^{-1}$ (Fig. 2a) (Boldrin et al., 2005; Palinkas et al., 2005; Wheatcroft et al., 2006). A rapid-response cruise was organized to collect sediment cores along and across the Po prodelta in December 2000 to understand the initial deposition of the flood deposit. The stations were re-occupied eight times over the next 2 years by an international team of American and European scientists as part of the EuroSTRATAFORM project, in order to capture the temporal evolution of the initial flood deposit. Results from this international effort were published in several manuscripts (Fox et al., 2004; Boldrin et al., 2005; Palinkas et al., 2005; Syvitski et al., 2005a; Wheatcroft et al., 2006; Milligan et al., 2007; Miserocchi et al., 2007) and they will be used in this study to better constrain our results. In order to be consistent with the previous published studies, we kept the same station locations occupied during the EuroSTRATAFORM project.

2.2 The May 2009 flood event

The May 2009 flood was triggered by the combination of spring snow melting with a western perturbation coming from the Atlantic ocean. The winter 2008–2009 was particularly wet allowing for the significant accumulation of snow on the Alps (Fig. 1a). This water reservoir was subsequently released because of the temperature raising since mid-April. At the end of April, heavy precipitations occurred in the Po watershed, mainly in the western portion of the drainage basin. The coexistence of rainfall and snowmelt resulted in increasing the river flow that reached the peak on 2 May (Fig. 2b).

BGD
7, 7849–7902, 2010

Figure 2b shows the Po river discharge at Pontelagoscuro gauging station from June 1999 through June 2000 and from October 2008 through October 2009. Although inferior to the October 2000 flood, the May 2009 event was significant reaching over 8000 $m^3 s^{-1}$ (Fig. 2). These two floods exhibited interesting contrasts and similarities. First of all, these floods occurred during different seasons and were triggered by different events (i.e. rainfall for the October 2000 flood whereas combination of snowmelt and rainfall for the May 2009 flood). Then, whereas the October 2009 flood was a discrete event, the May 2009 flood occurred at the end of the most rainy period of the last century recorded in the Northern Italy (Nanni et al., 2009). As a result, the May 2009 flood was preceded by at least 8 important events exceeding 4000 $m^3 s^{-1}$ (Fig. 3b). Concerning the similarities, the flood emplacement in May 2009 occurred during fair marine weather conditions (wave height <1 m) and relative small tide oscillations (~50 cm) (Fig. 3b, c) suggesting deposition in shallow regions of the prodelta as observed for October 2000 flood (Wheatcroft et al., 2006).

3 Methods

3.1 Sampling

3.1.1 Suspended material of the Po river

Suspended sediments from the Po river were collected on 23 April 2009 at Pontelagoscuro gauging station during a peak in water discharge (~5000 $m^3 s^{-1}$, H event in Fig. 2b). Samples were collected from a bridge in three different locations, nominally left, center, and right relative to the river axis. Three subsamples (50 ml) from each sample (25 liters) were filtered on pre-combusted and pre-weighted GF/F filters (0.7 µm mesh). Filters were oven-dried (50 °C) for 24 h and weighted to calculate the suspended sediment concentration (SSC, mg l^{-1}). Subsequently, remaining water samples were filtered with a 63 µm mesh. The fraction >63 µm was placed in the

BGD
7, 7849–7902, 2010

oven (50 °C) and then weighted to calculate the coarse fraction. The remaining water samples (<63 µm) were placed in the dark at 3 °C for 3 days until complete settling of particles. The supernatant was removed and a subsample was filtered on precombusted GF/F filter to estimate the remaining material in suspension. This latter fraction was less than 0.1% relative to the SSC for each sample. The fraction <63 µm was transferred in plastic tubes and then centrifugated. The supernatant was removed and tubes were placed in the oven (50 °C). Both coarse and fine fractions were grind and used for organic carbon (OC), total nitrogen (TN), and OC stable isotope (δ^{13}C), and biomarkers analyses.

3.1.2 Suspended material in the Po prodelta

Because of distance between Pontelagoscuro gauging station and the river mouths, the time elapsed for the water to reach the sea must be taken into account. Considering a current speed of 2–3 m s^{-1} during flood events (Brunelli et al., 2006) and the distance of ~90 km from Pontelagosuro to Pila mouth, the theoretical river discharge at Pila mouth was calculated adding 12 h to the Pontelagoscuro discharge (Fig. 3a). This 12 h offset was considered as a conservative estimate. Throughout the text, discharge data always refer to these theoretical values at Pila mouth unless specified.

Suspended materials in the Po prodelta were collected during two periods of the May 2009 flood, including early in the event under conditions of moderate river flow on 29 April (~4500 m^3 s^{-1}) and 24 h later during peak discharge on 1 May 2009 (~8000 m^3 s^{-1}) (Fig. 3a). Top and bottom water samples were collected on the R/V *Urania* using a CTD Rosette systems equipped with Niskin bottles. At each station, continuous profiles of salinity, transmittance, and fluorescence were obtained using a Sea-Bird CTD profiler (Mod. SBE 911 *plus*). Top and bottom water samples were sampled at ~1 m below sea surface and ~2 m above seabed, respectively. Water samples were filtered on pre-combusted and pre-weighted GF/F filters (two replicates) and Isopore Membrane polycarbonate filters (0.4 µm mesh, 142 mm diameter). GF/F filters were rinsed with MilliQ water and oven-dried (50 °C) on ship. GF/F filters were used

BGD
7, 7849–7902, 2010

for SSC, organic carbon (OC), total nitrogen (TN), and carbon stable isotope analyses ($\delta^{13}C$). Polycarbonate filters were placed in large plastic tubes with 50 ml of filtered seawater. Tubes were capped and vigorously shacked until complete of detachment of material from the filter. Filters were then rinsed with filtered seawater and removed from the tube. Tubes were centrifuged, the supernatant removed with a syringe and the recovered sediment was oven-dried (50 °C) on ship. Once dry, samples were grind for biomarkers analyses. An aliquot of unfiltered suspended material was used for grain-size analyses.

3.1.3 Sediment cores

During the Eurostrataform project (Palinkas et al., 2005; Wheatcroft et al., 2006; Miserocchi et al., 2007) sediment cores were collected in the Po prodelta to describe the initial emplacement of the October 2000 flood. Stations were then re-occupied 8 times in the following 2 years to follow the evolution of the flood deposit through time. In this study, sampling targets were identical to the stations occupied during the Eurostrataform project to be consistent with previous publications.

Sediment cores were collected before and after the peak discharge. The first set of samples were collected on 30 April and 1 May when the flow ranged from ~6000 to ~7000 $m^3 s^{-1}$ (Fig. 3a). The second set of samples were collected on 5 May when the discharge dropped to ~5000 $m^3 s^{-1}$. Sediment cores were collected using a box-corer. On deck, sediments were sub-sampled for x-radiographs, biogeochemical, and ^{7}Be analyses using slabs and PVC tubes. Samples for x-radiographs and biogeochemical analyses were placed in the dark at 3 °C. On board, sediment cores for radioisotope analyses were extruded, sub-sampled at 1 cm interval, and placed in the oven. In the laboratory, rectangular containers were x-radiographed and then sub-sampled at 1 cm intervals for biogeochemical analyses. Samples were then oven-dried (50 °C).

BGD
7, 7849–7902, 2010

3.2 Analyses

3.2.1 SSC, OC, TN, and $\delta^{13}C$

SSC, OC, TN, and $\delta^{13}C$ were calculated as mean of two replicates for each sample. In the laboratory, pre-weighted GF/F filters were oven-dried (50 °C) to ensure complete removal of moisture. Two filters for each sample were then weighted to calculate the total suspended matter (SSC, mg l^{-1}). Linear regression was used to convert transmittance data in SSC values. However, because during the peak discharge the trasmissometer reached the bottom scale (0%), SSC and transmittance do not exhibit a robust relationship.

OC, TN, and $\delta^{13}C$ analyses were carried out on acidified GF/F filters and sediment samples (HCl, 10%) to remove the inorganic fraction. Analyses were performed using a Thermo Electron DeltaPlus XP mass spectrometer directly interfaced to a Costech ECS4010 Elemental Analyzer via a Conflo III. The internal standards for isotopic measurements were apple leaves (NIST 1515) and the error for replicate analyses of the standard was ±0.05‰. OC and TN values are reported as weight percent (wt%) whereas stable isotope data are expressed in the conventional delta notation (δ).

3.2.2 Terrigenous biomarkers

Alkaline CuO oxidations were carried out using a Microwave digestion system according to the procedure described in Goñi and Thomas (2000). Dry samples were placed in teflon vessels with 15 ml of alkaline solution (2N NaOH), 500 mg of CuO, 50 mg of $Fe(NH_4)_2(SO_4)_2{\cdot}6H_2O$ and oxidized for 1.5 h at 150 °C. Once the oxidation was complete, a known amount of recovery standards (ethylvanillin and trans-cinnamic acid) was added to each vessel and acidified to pH 1 with HCl. Reaction products were extracted with ethylacetate and then evaporated to dryness under N_2. Once the solvent was evaporated, samples were re-dissolved in pyridine. Terrestrial OC yields a suite of lignin reaction products including vanillyl phenols (V-series), syringyl phenols

BGD
7, 7849–7902, 2010

(S-series), and cinnamyl phenols (C-series). Throughout the text, Λ refers to the carbon-normalized sum of lignin phenols (V + S + C). Reaction products were analyzed as trimethylsilyl derivatives (BSTFA reagent) by gas chromatography (GC) using a Hewlett-Packard 5980. The yields of individual lignin and non-lignin oxidation products were quantified by GC-MS using selective ion monitoring. The compounds were separated chromatographically in a 30 m × 250 µm DB1 (0.25 µm film thickness) capillary GC column, using an initial temperature of 100 °C, a temperature ramp of 4 °C/min and a final temperature of 300 °C. Phenols biomarkers were quantified using the response factors of commercially available standards whereas Cut, FA, and DA quantifications were accomplished by comparing the response factor of trans-cinnamic acid (Goni et al., 1998).

3.2.3 Surface area, sediment texture, and Coulter Counter data

Approximately 5 g of unground, salt-free sediment samples were combusted at 400 °C for 3 h to remove organic matter. The surface area of sediment samples were determined by nitrogen adsorption, using a 5-points BET method. About 1 g of pre-treated sediment was degassed at 300 °C in the vacuum station to ensure complete removal of moisture prior to analysis on Micromeritics surface area analyzer TriStar 3000. Data are reported as $m^2\,g^{-1}$ sediment. The remaining OC-free sediment samples were used for grain-size analysis. Samples were dispersed in sodium metaphosphate and then sieved with a 125 µm prior to analysis on Micromeritics SediGraph 5120. Data are shown as median value in µm (D_{50}) and relative contribution to dry weight for clay (<3.9 µm), silt (3.9–62.5 µm), and fine sand (62.5–125 µm). Suspended samples for particle concentration and grain size spectrum were processed on board, immediately after sampling, using a Multisizer 3 Coulter Counter, equipped with a 100-µm aperture tube, sizing particles from 2 to 60 µm in diameter. Data are shown as grain size spectra and median value (D_{50}) in µm.

BGD
7, 7849–7902, 2010

3.2.4 ^{7}Be

Dried samples were slightly disaggregated, then put in plastic jars and counted by gamma spectrometry in an identical counting geometry. Gamma emissions were counted at 477.7 keV photopeak for approximately 24 h using Ortec germanium detectors which were calibrated with commercially available standard. Activities were then decay-corrected to the time of collection.

3.2.5 Biogenic opal

Biogenic opal ($SiO_2 \times nH_2O$) content was measured in sediment samples according to the procedure described in De Master (1981). About 90 mg of sediments were placed in Teflon tubes. Alkaline digestion was performed with 40 ml 0.5 M Na_2CO_3 solution at 80 °C for 5 h. At known intervals, Teflon tubes were centrifuged and the supernatant was sub-sampled (200 µl). Dissolved silica was then measured with the molybdate-blue spectrophotometric method (wave length 812 nm). Dissolution kinetic of quartz is lower relative to biogenic opal dissolution although it might increase the concentration of silicic acid in the supernatant with time. Therefore, the intercept of the regression line between time (x) and silica concentration (y) was considered as the actual biogenic opal content (Mortlock and Froelich, 1989). Data are reported as weight percent (wt%) of SiO_2.

3.2.6 Radiocarbon measurements

Radiocarbon analyses were performed at the National Ocean Sciences Accelerator Mass Spectrometry Facility (NOSAMS, Woods Hole Oceanographic Institution). The CO_2 samples were obtained by the combustion of bulk OC from pre-acidified samples to remove the inorganic fraction. The gas was then purified cryogenically and converted to graphite using hydrogen reduction with an iron catalyst. The graphite was pressed into targets, which were analyzed on the accelerator along with standards and

BGD
7, 7849–7902, 2010

process blanks. Oxalic Acid II (NIST-SRM-4990C) was the primary standard used for all ^{14}C measurements. Radiocarbon measurements results are reported as $\Delta 14C$ (‰).

3.3 Statistical analysis

Differences between groups were performed using a two-tailed unpaired *T*-test. Alpha levels were set to 0.05 (significant) and 0.01 (highly significant). *P* values are shown throughout the text when difference are statistically significant.

4 Results

4.1 Po river suspended matter

Results for river samples are listed in Tables 1, 2. Most of the sediment load in the river was associated with the fine fraction (<63 µm) accounting for over 97% of the SSC. Coarse and fine fractions exhibited contrasting compositions statistically significant ($p < 0.01$) in both bulk and biomarker parameters. On average, the coarse fraction showed higher OC and TN contents, relatively depleted $\delta^{13}C$ values, and higher OC:TN ratios. Fine material was less rich in OC and TN, isotopically heavier, and depleted in OC relative to TN compared to the coarse fraction. Radiocarbon measurements were carried out only on samples collected in the center of the river. $\Delta^{14}C$ of the fine fraction was significantly more depleted than the coarse material. All carbon-normalized lignin-derived products (i.e., syringyl, vanillyl, and cinnamyl phenols) were more abundant in the coarse fraction relative to the fine material ($p < 0.01$). The cinnamyl to vanillyl phenols ratio ([C:V]) and the syringyl to vanillyl phenols ratio ([S:V]) have been used in several biogeochemical studies to infer the origin of terrigenous tissues (e.g., angiosperm, gymnosperm, woody, and grass tissue) (Hedges and Mann, 1979; Hedges et al., 1986; Goni et al., 1998, 2008; Gordon and Goni, 2003). In addition, the acid to aldehyde ratios of vanillyl ([Vd:Vl]) and syringyl ([Sd:Sl]) phenols

BGD
7, 7849–7902, 2010

provide additional details concerning the degradative stage of terrigenous OC (Opsahl and Benner, 1995; Onstad et al., 2000; Gordon and Goni, 2003; Goni et al., 2008). Only the [C:V] and [Vd:Vl] ratios exhibited significant differences between coarse and fine materials ($p < 0.05$). ^{7}Be was measured and detected in all fine materials whereas coarse fractions were not enough for radioisotope analyses.

4.2 Water column in the Po prodelta

Results for the water column are shown in Figs. 4–5 and Tables 3, 4, 5. Samples were grouped according to latitude in three sub-regions: north, central, and south. The north region is under the influence of Pila outlet whereas the central and south prodelta are affected by Tolle and Gnocco/goro distributary, respectively. During moderate discharge when the flow was ~5000 $m^3 s^{-1}$, salinity, transmittance and SSC values showed weak evidence of plume intrusion (Table 3; Figs. 5, 6). In surface waters, the highest SSC and lowest transmittance values were observed in the north prodelta under the influence of Pila distributary (Fig. 3; Tables 4, 5). Conversely, resuspension dominated in both center and south prodelta where bottom waters exhibited low transmittance and relatively high SSC values likely as result of a storm event that occurred the day before sampling (wave height >3 m) (Fig. 3c). This turbid nepheloid layer was measured several meters above the seafloor (Fig. 5) and was characterized by a fine sediment texture (Table 3). During the peak of the flood when the discharge reached ~8000 $m^3 s^{-1}$, surface waters exhibited an overall decrease in salinity and transmittance values as well as an increase in the SSC values in particular next to the river outlets in the north and central prodelta (E and J transect, respectively). As a result, all aforementioned parameters exhibited statistically significant differences ($p < 0.05$) between moderate and peak discharge in all sub-regions, except for the sediment texture. Although the influence of the flood was observed in all sub-regions, the southern prodelta exhibited a relatively modest increase in SSC values (max value at P15 station, 5.7 mg/l). The rest of the prodelta exhibited a significant increase in the SSC values, especially just off Pila (E16 station, 53.1 mg/l) and Tolle (J13 station, 26.5 mg/l)

BGD
7, 7849–7902, 2010

mouths in the north and central prodelta, respectively (see Fig. 1 for site locations). Conversely, the highest fluorescence values ($p < 0.01$) were observed in the south prodelta in both river discharge conditions, in particular during the peak of the flow (Table 2 and Fig. 6).

The weight percent (wt%) of OC and TN exhibited a broad range of values in the prodelta, ranging from 1.7 to 11.7% and from 0.24 to 2.26% for OC and TN, respectively. The highest OC and TN concentrations were mainly measured during moderate flow far from distributary mouths. No statistically significant differences were observed in the elemental compositions between moderate and peak discharge (Table 4). However, because of high sediment concentrations during the peak of the flow, surface waters exhibited higher concentrations of OC and TN per liter (µg/l) relative to the moderate discharge condition ($p < 0.01$). $\delta^{13}C$ did not exhibit a clear spatial distribution in the prodelta and no statistically significant differences were observed between sampling periods. Lignin phenols were measured in all suspended samples, although their concentrations showed a broad range of values from 0.07 to 1.61 mg/100 mg OC. Differences in the concentration of lignin phenols were observed between moderate and peak discharge ($p < 0.05$) in surface waters (Table 5). The highest Λ values were measured during the peak of the flow just off Pila (E transect) and Tolle (J transect) mouths, which is consistent with the SSC values.

4.3 Sediment cores

^{7}Be data and radiographs for sediment cores collected in the Po prodelta are shown in Table 6 and Fig. 6. Samples were grouped based on the date of collection. Thickness of the October 2000 flood (Wheatcroft et al., 2006) is included in Table 6 for comparison. Most of the cores collected before the peak of the flood did not show any clear evidence of recent sediment deposition (Fig. 6). ^{7}Be penetrations were relatively modest and most of the cores were bioturbated. Only samples collected off the Pila mouth (E transect) showed significant ^{7}Be penetrations (from 1 to 10 cm), suggesting recent deposition attributable to the late April–early May flood or, alternatively, to

BGD
7, 7849–7902, 2010

previous events. Unfortunately, ^{7}Be is not sufficient to exactly assess when accumulation occurred as this radionuclide is theoretically detectable up to ~200 days since sediment emplacement. ^{7}Be penetrations in the central prodelta (J and H transects) were extremely low (1–2 cm), particularly evident when these estimates are compared to the October 2000 flood thicknesses (Table 6). In the southern prodelta, ^{7}Be was not detected as at the N14 station (i.e. 0 cm ^{7}Be penetration).

Stations under the influence of Pila and Tolle distributaries have been reoccupied after the peak discharge on 5 May 2009. These two sites exhibited among the highest SSC and lowest transmittance values measured in surface waters on 1 May 2009 during the peak of the flood (Fig. 4). Radiographs indicated thick event strata up to 17 and 6 cm for E16-II (Pila) and J13-II (Tolle), respectively (Fig. 6). Comparing ^{7}Be penetrations and radiographs before and after the peak discharge, the emplacement of these event strata are undoubtedly the result of the May 2009 flood. Both flood deposits are characterized by coarse basal strata wherein ^{7}Be was not detected, probably as a result of preferential adsorption of the radionuclide on fine fractions. Active bioturbation was noticed during the subsampling of the E16-II core and it was then confirmed by the radiograph; however, most of the strata were preserved. Both sediment cores collected after the peak of the flood on 5 May (E16-II and J13-II cores) were used to characterize the OC deposition as result of the May 2009 flood. For this purpose, only event-strata belonging to the May 2009 event were analyzed and discussed in this study (first 17 and 6 cm for E16-II and J13-II, respectively).

Although event-strata collected in the north and central prodelta are the result of the same flood event, E16-II and J13-II cores exhibited significant differences in several parameters. Among sedimentological variables, the E16-II core was significantly coarser and exhibited lower SA compared to the J13-II core ($p < 0.01$) (Table 7). Concerning bulk biogeochemical parameters, statistically significant differences included the OC loading as well as the δ^{13}C ($p < 0.01$) (Table 7). Specifically, E16-II showed a higher OC loading and more depleted δ^{13}C values. Both cores exhibited an increase in the δ^{13}C that coincided with the basal silty-sandy layer where ^{7}Be was not

BGD
7, 7849–7902, 2010

detected. Down-core profiles of $\Delta^{14}C$ in both cores were relatively similar. In the upper core, $\Delta^{14}C$ values were relatively enriched compared to the silty-sandy stratum where ^{7}Be was not detected. Significant differences ($p < 0.001$) were observed in the concentration of syringyl, vanillyl, and cinnamyl phenols, all of which were relatively more abundant in the E16-II core (Table 8). In spite of these differences in lignin contents, lignin-based parameters such as [C:V], [S:V], [Sd:Sl], and [Vd:Vl] were fairly comparable between cores indicating a terrigenous composition relatively homogeneous between north and central prodelta. Conversely, statistically significant differences ($p < 0.01$) were observed between sediment cores and suspended samples for all aforementioned lignin-based parameters.

Given that extremely low SSC were measured in the southern prodelta on 1 May despite the peak discharge, coring targets in this region were not re-occupied after the peak of the flood. However, the sediment core collected just off the Gnocca outlet (core N14, see Fig. 1) on 29 April was used as a stratigraphy record to characterize the event-driven supply of OC in the southern prodelta during the most rainy period of the last century that resulted in 8 distinct flood events (Fig. 2b). In addition to ^{7}Be and radiographs, bulk measurements were carried out on this core and they will be compared to biogeochemical compositions of a flood deposit collected at the same station two months after the peak of the October 2000 flood (Miserocchi et al., 2007). The N14 radiograph indicated a highly bioturbated sediment fabric with no evidence of layering and no detectable ^{7}Be (Table 6; Fig. 6). SA down-core profile was relatively homogeneous, consistent with the bioturbated profile (Fig. 7). Only the major bulk measurements were carried out in this core. OC and TN contents were significantly lower than event-strata collected in the same station after the October 2000 flood ($p < 0.01$). In addition, the $\delta^{13}C$ that was isotopically heavier ($p < 0.01$) relative to the October 2000 deposit suggesting a different OC composition (Table 7).

BGD
7, 7849–7902, 2010

5 Discussion

5.1 Moderate vs. high discharge

Based on seabed grain size distributions, Milligan et al. (2007) explained the particle settling from the Po plume as a function of the river discharge. During low-to-moderate flow conditions, sediment deposition is rapid and occurs within 2 km from the river mouth (<10 m water depth). Such a rapid settling is caused by flocculation processes and relatively short floc residence time within the thin surface plume. Conversely, during high discharge levels, sediments are transported further into the prodelta because a thick plume increases the residence time of particles in the water column (i.e. sediment buoyancy) .

In our study, the aforementioned conditions described by Milligan et al. (2007) were observed 24 h apart from each other (Figs. 4, 5). During the first survey on 29 April when the river flow was ~5000 $m^3 s^{-1}$, SSC values in surface waters were relatively low (mean value 3.8 ± 2.2 mg/l, Table 3) and did not differ from SSC values measured by Boldrin et al. (2005) during dry periods (mean value 4.4 ± 2.8 mg/l at ~1000 $m^3 s^{-1}$; Boldrin et al., 2005). Indeed, the surface plume was relatively thin, whereas the highest SSC were observed in bottom waters (5.5 ± 3.4 mg/l, Table 3) because of a storm-driven resuspension event occurred a day before the cruise on 28 April (Fig. 5). During the second survey, on 1 May when the river flow increased to ~8000 $m^3 s^{-1}$, the turbid plume extended further into the prodelta, such as observed in the Tolle region and significant settling of sediment from the surface plume was observed near the Pila mouth (Figs. 4, 5). Conversely, the southern prodelta under the influence of Goro/Gnocca outlets exhibited a relatively small increase in SSC despite the marked decrease in salinity (Table 2). It is well established that the supply of fresh water from the southern distributaries during flood events is significant and accounts for ~40% of the total fresh water entering the delta. Therefore, the combination of having low salinities and relatively low material in suspension (Fig. 5) suggested that southern distributaries supplied a significant amount of fresh water while most of their particulate supply was trapped in

BGD
7, 7849–7902, 2010

the shallow prodelta because of flocculation and settling processes. Alternatively, a fraction of sediment load could have settled even before reaching the sea within the distributary channels (Fox et al., 2004). Indeed, based on published data for the Goro distributary, Syvistki et al. (2005b) estimated a net sediment accumulation along this southern channel, accounting for 16% of the total annual sediment entering the delta. The authors calculated sediment deposition rates for the Goro channel that range from 4.7 to 5.7 cm y^{-1}. These values are higher than sedimentation rates measured in most of the subaqueous prodelta (Frignani et al., 2005). As a result, the Goro channel floor is becoming super-elevated compared to the surrounding delta flood plain (Syvistki et al., 2005b).

Since SSC in surface waters did not exhibit any statistical difference between dry periods (Boldrin et al., 2005) and moderate discharge, our results suggest that there must be a threshold level for the river discharge after which the plume can ultimately penetrate into the prodelta. Based on differences in SSC and transmittance values observed between moderate and peak discharge, this threshold level has to be between ~5000 and ~8000 $m^3 s^{-1}$. However, the SSC values during the peak discharge were still lower than expected suggesting that even the second sampling carried out on 1 May did not fully represent the settling and emplacement mechanisms described by Milligan et al. (2007) with the exception of the region just off the Pila mouth. According to the authors, event-layers deposition occurs directly from the surface plume because of flocculation and settling processes occurring in the turbid plume. Since sediment settling was observed in the north mouth (Fig. 5, peak discharge), our results suggest that in the central and southern distributaries the flow was still not sufficient to keep in suspension the flocculated material along channels. As a result, it is likely that in these regions most of the sediment supply was trapped in shallow waters and/or within distributary channels.

It is also important to highlight, that there are other unknown variables such as sediment availability that may affect the land-ocean exchange of particulate material in a multi-channel setting. Specifically, the aforementioned threshold level might change

BGD
7, 7849–7902, 2010

depending on the intervals between floods, which allows sufficient time for channels to accumulate new sediment that will be subsequently remobilized during floods. In this aspect, the October 2000 flood was extremely different from the May 2009 flood, not only because of the flood magnitude and duration, but also because the October 2000 flood was a discrete event whereas the May 2009 flood was at the end of a series of flood events (Fig. 2).

5.2 Accumulation in the subaqueous delta during ordinary floods

Indirect evidence from sediment cores support our hypothesis that most of the sediment supply to the subaqueous prodelta occurs mainly when the river experiences particularly intense and extensive flood events. Figure 6 shows sediment cores collected in the Po prodelta after the highest precipitation period recorded over the last century that resulted in a series of flood events between 4000 and 6000 $m^3 s^{-1}$ (8 events, Fig. 2b). However, in spite of the relatively high river flow, most of the cores collected did not show clear evidence of recent deposition. The north prodelta just off the Pila mouth (E transect) exhibited relatively high ^{7}Be penetrations and evidence of laminated beddings in shallow water (i.e., E11 core). However, thicknesses were extremely small compared to the October 2000 flood that resulted in a thick deposit in the same stations (Table 6) (Wheatcroft et al., 2006). The rest of the cores collected in the prodelta showed bioturbated sediment fabric and extremely low ^{7}Be penetrations, such as in the central prodelta (1–2 cm), or even no detectable ^{7}Be, such as in the south prodelta at the N14 station. If considerable sediment deposition had occurred in the subaqueous prodelta as a result of these eight ordinary flood events preceding the May 2009 flood, we should have observed significant penetrations of ^{7}Be and/or seen laminated beddings. For example, indications of event-strata preservation of the October 2000 flood were observed throughout the prodelta by means of radiographs and ^{7}Be inventory several months after the flood and in some stations up to two years since the flood emplacement (Palinkas et al., 2005; Wheatcroft et al., 2006). Therefore, the relative modest deposition in the subaqueous prodelta – despite the numerous events

BGD
7, 7849–7902, 2010

– suggests that the material delivered during ordinary floods (2–3 y return periods) is mainly trapped in shallower waters or within distributary channels (Fox et al., 2004), whereas during large flood events, such as the October 2000 flood, sediments can efficiently reach the subaqueous delta. This does not necessarily imply that sedimentation does not occur during ordinary floods. Some of the material probably accumulates on seabed in the prodelta, but the thicknesses of these deposits are probably not enough to compete with post-depositional processes such as bioturbation and wave-supported sediment transport.

The effect of ordinary vs. large floods on the terrigenous OC burial was particularly marked in the southern prodelta. In this region, about two months after the peak of the October 2000 flood, a 12-cm thick event-stratum was observed at the station N14 based on radiographs and ^{7}Be penetration (Palinkas et al., 2005; Wheatcroft et al., 2006). In addition, the first 10 cm of this sediment core showed relatively depleted δ^{13}C values, indicating deposition of fresh terrigenous OC at the top of the core (Miserocchi et al., 2007). The same target was reoccupied in May 2009 and, although the river experienced 8 floods from November 2008 through May 2009, the sediment core was highly bioturbated and lacked ^{7}Be activity (i.e., 0 cm of ^{7}Be penetration) (Fig. 6; Table 6). Furthermore, the δ^{13}C did not show any evidence of deposition of fresh terrigenous OC at the upper core (Fig. 7). These results were somehow unexpected since it is well established that ~40% of the fresh water supplied during floods occurs via southern distributaries. Therefore, the paradox that a significant amount of fresh water entered the southern delta during flood events, without showing evidence of recent deposition in the stratigraphy record, supports, once again, the hypothesis that most of the material delivered during ordinary floods by the southern distributaries is trapped in shallow regions and/or within the distributary channels, consistent with water column results. Consequently, sediment accumulation in this location is driven by other mechanisms including southerly current events forced by winds and wave-supported turbidity flows, as suggested by modeling and in-situ tripod measurements (Traykovski et al., 2007). Therefore, most of the accumulated material in the southern prodelta

BGD
7, 7849–7902, 2010

is likely reworked material whose bulk composition is significantly different from fresh terrigenous OC (Fig. 7).

5.3 The May 2009 flood deposit

Although Pila and Tolle belong to the same channel network, their outlets exhibit contrasting geomorphologic features. In the north region, the prodelta experiences significant progradation resulting in a seaward migration of the Pila outlet (river-dominated delta) (Fig. 1) (Correggiari et al., 2005). Conversely, in the central prodelta, wave-energy dominates on the river supply generating a typical estuary-like river mouth characterized by sandy barriers (wave-dominated delta) (Fig. 1) (Correggiari et al., 2005). Stations off Pila and Tolle mouths were re-occupied after the peak of the flood on 5 May. Core E16-II was collected in the north prodelta whereas core J13-II was taken in the central region. These sites were re-occupied because they exhibited among the highest SSC values measured in the surface plume on 1 May during the peak of the flood. Comparing radiographs and ^{7}Be penetrations before and after the peak discharge, we estimated event-layers 17 and 6 cm thick in the north and central prodelta, respectively. Deposition in the Pila region was expected based on settling and flocculation processes observed during the peak on 1 May (Fig. 5). Conversely, settling from the surface plume was not detected on 1 May suggesting that conditions sufficient to cause accumulation in this central region were likely reached the subsequent day since the peak of the flood lasted for two days. Therefore, besides absolute peak discharge, the length of the flood is clearly another factor that enhances the plume thickness that in turn increases the residence time of particles within the turbid plume allowing for the deposition in the subaqueous prodelta.

It is worth to highlighting that in addition to having a different thickness these event-strata displayed significant differences in the sediment texture (Fig. 8a, b). Grain-size distribution in two intervals from each core was used to examine these differences (Fig. 9a). Bimodal grain-size distribution was observed in the flood deposit collected in the north prodelta (E16-II). For the most part of this core, the most frequent size classes

BGD
7, 7849–7902, 2010

were at the silt-clay boundary (~4 μm) and in the silt fraction (~35 μm). Conversely, the flood deposit collected in the central prodelta (J13-II) exhibited a normal distribution centered at the silt-clay size boundary (~4 μm). The missing peak in the silt fraction for this latter core indicates that settling of silty material occurred prior to reaching the central subaqueous delta. Such process might have occurred within the Tolle branch and/or at the channel outlet. Indeed, the geomorphologic architecture of Tolle mouth, characterized by an estuary-like setting (Fig. 1), suggests that the material enters the Adriatic Sea via this distributary as a buoyancy-driven plume rather than a momentum-driven flow (Syvitski et al., 2005a). As a result of the reduced transport capacity, the coarse material is selectively trapped prior to reaching the sea within the Tolle mouth.

Particle size distribution in surface samples (~1 m below the sea surface) collected above E16 and J13 stations highlights similar spatial differences (Fig. 9b). Specifically, in both moderate and peak discharges, the north prodelta exhibited a coarser sediment texture in suspended sediments relative the central region. In addition, since the particle size distribution remained fairly constant with time, these results might imply that sediment texture in the surface plume is mainly driven by the delta architecture rather than the discharge extent.

5.4 OC composition within flood deposits

Fine and coarse suspended sediments collected during the H event (Fig. 2b) in the Po river displayed contrasting compositions in both bulk and biomarker parameters (Tables 1, 2). Specifically, coarse fraction exhibited higher OC:TN ratios, relatively depleted $\delta^{13}C$, significantly higher lignin contents, and a younger ^{14}C age. Based on these differences, we can conclude that the OC in the coarse fraction (>63 μm) was primarily composed of relatively young organic plant detritus, whereas the fine fraction (<63 μm) was mainly affected by aged, humified OC bound to the mineral soil.

Event-strata collected in the north (E16-II) and central prodelta (J13-II), in addition to having a distinct grain-size, showed contrasting OC compositions concerning Λ and $\delta^{13}C$ ($p < 0.01$) (Fig. 8c, g). This analogy suggests that coarse and fine particles

BGD
7, 7849–7902, 2010

display a different composition as much as coarse and fine fractions of river samples. However, the OC loading in both deposits are within the range of the mono-equivalent layer (Mayer, 1994), indicating that most of the OC is associated with the mineral matrix of inorganic particles (Fig. 8f). Therefore, rather than mixing of matrix-free vascular plant detritus with soil-derived OC, as seen for river samples, differences between flood deposits might be the result of diverse OC coated on different particles (i.e., organo-clay complexes vs. organo-silt complexes). Besides OC loading, other parameters pointed toward similar conclusions. For example, in both flood deposits OC:TN ratios are within the range of soil-derived OC (Hedges and Oades, 1997). In parallel, radiocarbon measurements indicated an aged OC source rather than a fresh vascular plant detritus (Fig. 8d, c). In addition, proxy for microbial degradation of terrigenous OC such as the acid to aldehyde ratios of the vanillyl ([Vd:Vl]) and syringyl ([Sd:Sl]) phenols do not indicate any differences between deposits, consistent with elemental and radiocarbon results (Table 8). It is also important to highlight that granulometric classes of the coarse and fine material for suspended river sampled and flood deposits are not identical. Suspended river material was sieved with a 63 µm mesh to separate the mud (clay + silt) from the sand fraction whereas most of the differences between flood deposits were due to a diverse proportion of silt (4–63 µm) and clay (<4 µm). Therefore, results from the size fractionation of river samples can not be directly apply to flood deposits. It is also interesting to observe that both flood deposits had a sandy-silty basal stratum that, despite it showed a significant contribution of sand, had a divergent composition relative to the coarse fraction collected in the river. These coarse basal strata had relatively old radiocarbon ages, low OC:TN ratios and displayed an enriched $\delta^{13}C$ compositions. Therefore, the terrigenous OC mixing within a flood deposit is probably more complex than a simple mixture of coarse material, relatively rich in modern vascular plant detritus, with fine material, relatively rich in aged, humified soil-derived OC. Indeed, another important and unknown element that should be considered is the chance that a certain fraction of the material accumulated in the prodelta throughout the flood was resuspended sediment from the channel floor. However, since ^{7}Be in

BGD
7, 7849–7902, 2010

sediments deposited along channel floor for more than ~200 days should have decayed (Svendsen et al., 2009), we can at least assess that most of the material was fairly recent as ^{7}Be was detected in both sediment cores.

Finally, dilution with lignin-free organic matter in the central prodelta (J13-II core), such as algal material, might explain the lower lignin contents as well as the enriched δ^{13}C values. However, opal contents in the event-strata does not support the hypothesis of autochthonous OC burial being particularly significant in the Tolle region (Fig. 8h). If significant algal burial had occurred in the central prodelta, we should have measured relative higher opal contents in this area as diatoms constitute the predominant fraction of autochthonous production in the Po prodelta (Aubry et al., 2004).

5.5 OC sources in the surface plume and end-member mixing model

In prodelta regions, suspended particulate OC is a heterogeneous mixture of different compounds coming from different sources including vascular plant detritus, organic matter sorbed onto the surface of suspended particles, as well as eustuarine and marine phytoplankton (Hedges and Oades, 1997; Goni et al., 2003, 2008; Gordon and Goni, 2003; Tesi et al., 2007). As the aforementioned OC sources exhibit contrasting compositions, biogeochemical parameters such as OC, TN, δ^{13}C and Λ constitute a useful toolbox to infer the OC provenance. Average compositions of different OC sources are shown in Fig. 10 as boxes according to the literature (Hedges and Oades, 1997; Goni et al., 2003, 2005). At the top we have plotted river and prodelta samples to visually examine the influence of autochthonous and allochthonous OC sources on these samples.

Significant differences were observed between suspended material and sediment cores collected in the Po prodelta. Sediments were mainly affected by land-derived material, whereas autochthons production was the dominant OC source in suspended samples (Fig. 10). However, suspended samples collected during the peak discharge just off Pila and Tolle mouths exhibited a significant influence of terrigenous OC. A two end-member mixing model was used to quantify the influence of land-derived material

BGD
7, 7849–7902, 2010

and autochthonous phytoplankton in the surface plume. Previous studies in the Po prodelta have assessed the relative contribution of estuarine and marine phytoplankton using elemental compositions (OC/TN ratio) and $\delta^{13}C$ data (Boldrin et al., 2005; Giani et al., 2009). However, while the marine end-member can be assumed relatively stable in the model, the estuarine phytoplankton exhibits a broad range of $\delta^{13}C$ values (Goni et al., 2003). This occurs because the $\delta^{13}C$ signature of estuarine phytoplankton is driven by the relative mixing of fresh water (^{13}C depleted because of terrigenous biomass degradation) with seawater that is in equilibrium with the atmospheric pCO_2 ($\sim -8‰$). Therefore, for any given fresh-sea water mixture, the ^{13}C signature of the dissolved CO_2 changes affecting the isotopic signature of autochthonous phytoplankton (Hinga et al., 1994). For this reason, we preferred to group together estuarine and marine algae and apply a simple two end-member mixing model between autochthonous and allochthonous OC using TN:OC and Λ values (Fig. 11). The relative fraction of these sources have been assessed based on the position on the regression line ($r^2 = 0.87$) that includes surface suspended material collected in the plume and fine river samples (<63 µm) since the D_{50} in all suspended sediments were significantly lower than 63 µm (Table 3). Positions on the regression line were defined based on the minimum distance between samples and the regression line. Averaged value for the Po river fine fraction (<63 µm) was used as end-member for the material supplied by the river. As phytoplankton is a lignin-free OC source, the intercept for $\Lambda = 0$ was used to define the [TN:OC] value for the autochthonous end-member. The relative fractions of autochthonous and allochthonous sources were then converted in $\mu g\,OC\,l^{-1}$.

Figure 12 shows the results from the model. Samples were grouped in three sub-regions (i.e. north, central, south) according to the distance from the river mouths. Results are shown as mean and relative standard deviation for each sub-region. The relative fraction of autochthonous OC exhibited an overall increase with distance from the Pila mouth, especially during the peak of the flood. The concentration of allochthonous OC as $\mu g\,l^{-1}$ was slightly higher during the peak discharge, though these differences

BGD
7, 7849–7902, 2010

were not statistically significant. However, these similar concentrations indicate that phytoplankton growth was not limited by the increase in water turbidity, especially in the southern prodelta where we observed the highest autochthonous OC concentrations during the peak discharge consistent with fluorometer data (Fig. 5). During the peak of the flood, the relative fraction of allochthonous OC increased throughout the prodelta. Terrigenous material in the Pila region became the major OC whereas in the central and south prodelta allochthonous and autochthonous fractions were fairly even despite the high discharge. Concentration of land-derived OC as $\mu g\, l^{-1}$ were statistically higher during the peak of the flood relative to the early stage of the flood ($P < 0.01$). However, with the exception of the Pila region, central and southern prodelta exhibited terrigenous concentrations 1–2 fold less concentrated than the river ($5173 \pm 392\, \mu g\, OC\, l^{-1}$, Table 1) indicating that, despite the peak of the flood, flocculation and settling processes were still affecting the concentration of terrigenous OC within the plume.

5.6 Contrasts between event-strata and suspended materials

Concentrations of cinnamyl relative to vanillyl phenols ([C:V]) and syringyl relative to vanillyl phenols ([S:V]) provide details on vascular plant tissue origin. The [C:V] ratio is used to differentiate between woody and non-woody plants, whereas the [S:V] ratio is used to distinguish angiosperm from gymnosperm tissues (Hedges and Mann, 1979; Hedges et al., 1986). Coarse and fine fractions in suspended material collected in the Po river displayed relatively similar [C:V] and [S:V] ratios, despite the contrasting biogeochemical compositions. Only the [C:V] ratio exhibited statistically significant differences between fractions ($p < 0.05$) (Table 2), though mean values for the coarse and fine fractions were relatively close. Both [C:V] and [S:V] ratios were relatively similar between sediment cores collected in the north and central prodelta after the May 2009 flood (Table 8). This suggest that the relative proportion of lignin phenols is fairly homogeneous throughout the channels network as well as among different size fractions (i.e. silt vs. clay). However, both [C:V] and [S:V] exhibited statistically significant differences between suspended material and flood deposit ($p < 0.01$ and $p < 0.05$ for C:V

BGD
7, 7849–7902, 2010

and S:V, respectively) (Tables 5, 8). These ratios have been shown to be affected by degradation as well as leaching-adsorption mechanisms that increase the concentrations of cinnamyl and syringyl phenols relative to vanillyl phenols (Opsahl and Benner, 1995; Hernes et al., 2007). It is likely that both processes influenced the fine material in suspension within the surface plume and therefore these ratios should be carefully interpreted. In parallel, significant differences between suspended samples and sediment cores were observed in other lignin-based parameters such as [Vd:Vl] and [Sd:Sl] ratios ($p < 0.01$) (Tables 5, 8). These ratios have been used in several biogeochemical studies to assess the degradative status of terrigenous OC (Opsahl and Benner, 1995; Onstad et al., 2000; Gordon and Goni, 2003; Goni et al., 2008). However, the same leaching-adsorption processes affecting the [C:V] and [S:V] ratios have a similar effect on [Vd:Vl] and [Sd:Sl] ratios resulting in increasing the acid to aldehyde ratio. As a result, differences might not be driven by degradation processes, but rather leaching-adsorption mechanisms occurring in the surface plume.

6 Summary

This study investigated the event-driven supply and deposition of land-derived material in the Po prodelta characterized by a multi-channel architecture. The overall conclusion of this study is that the land-ocean exchange of particulate OC is not coherent throughout the channel network since each distributary channel behaves as an independent flood-dominated river. The followings are the specific findings:

1. Po river discharge exerts first-order control on the terrigenous OC concentration within the plume. Specifically, our results suggest the there must be a threshold level for the river discharge after which the land-derived OC plume can efficiently penetrate into the prodelta. Based on differences in suspended sediment concentrations measured in the surface plume during moderate and peak discharge, this level has to be between ~5000 and ~8000 $m^3 s^{-1}$. Below this value, most

BGD
7, 7849–7902, 2010

of the terrigenous OC is likely sequestered in shallow waters and/or within distributary channels. This trapping processes are particularly marked in the central and south prodelta where the flow through distributary-channels is not sufficient to compensate settling and flocculation processes even during relatively high discharge.

2. Similarly, results from sediment cores indicate that significant deposition in the subaqueous prodelta occurs only during particularly large flood events. During ordinary floods (between ~4000 and ~6000 $m^3 s^{-1}$) only a small fraction of material can reach the subaqueous delta. As a result, sediment accumulation is not sufficient to keep pace with post-depositional processes (e.g., bioturbation and storm-induced waves) resulting in a weak preservation of event-strata.

3. In both moderate and peak discharge, the relative fraction of terrigenous OC decreased with distance from the Pila distributary. In spite of this north-to-south decreasing, concentrations of allochthonous OC exhibited an overall increase throughout the prodelta because of the flood, especially in the north prodelta. In the southern prodelta, a thick stratum of fresh water characterized by relatively low SSC was observed during the peak of the flood. In this region, autochthonous OC was the main OC source consistent even during the flood. This suggests that settling processes, coupled with significant input of fresh water, are key factors for phytoplankton blooms during flood events in this region.

4. After the peak of the flood, a silty flood deposit was collected just off the Pila outlet in the north prodelta, while a muddy deposit was collected in front of the Tolle mouth in the central prodelta. Differences in grain-size were likely due to the estuary-like architecture of the central prodelta that caused trapping of relatively coarse material prior to reaching the sea. In addition, these flood deposits exhibited contrasting OC compositions including OC loading, $\delta^{13}C$, and lignin phenols concentrations. This analogy suggested that hydrodynamic sorting affected also the supply and deposition of terrestrially derived OC prior to reaching

BGD
7, 7849–7902, 2010

the subaqueous prodelta. In spite of these sorting processes, lignin-based parameters indicated that the composition of vascular plant tissues supplied to the prodelta is fairly homogenous throughout the channel network and between size-fractions.

Acknowledgements. The authors would like to acknowledge the FP7-Marie Curie Action who provided funding for this work under grant (SOMFlood project, Grant Agreement number: PIOF-GA-2008-221167). We also thank M. Claret Cortes, A. Gallerani, A. Remia, Y. Alleau, and J. Snyder for their help in the field and in the lab. Special thanks goes to the captain E. Gentile and to crew of the R/V *Urania*. This is contribution number 1700 of CNR-ISMAR, sede di Bologna.

References

Aubry, F. B., Berton, A., Bastianini, M., Socal, G., and Acri, F.: Phytoplankton succession in a coastal area of the NW Adriatic, over a 10-year sampling period (1990–1999), Cont. Shelf Res., 24, 97–115, 2004.

Berner, R. A.: Models for Carbon and Sulfur Cycles and Atmospheric Oxygen – Application to Paleozoic Geologic History, Am. J. Sci., 287, 177–196, 1987.

Berner, R. A.: Biogeochemical Cycles of Carbon and Sulfur and Their Effect on Atmospheric Oxygen over Phanerozoic Time, Global Planet. Change, 75, 97–122, 1989.

Blair, N. E., Leithold, E. L., Ford, S. T., Peeler, K. A., Holmes, J. C., and Perkey, D. W.: The persistence of memory: The fate of ancient sedimentary organic carbon in a modern sedimentary system, Geochim. Cosmochim. Ac., 67, 63–73, 2003.

Boldrin, A., Langone, L., Miserocchi, S., Turchetto, M., and Acri, F.: Po River plume on the Adriatic continental shelf: Dispersion and sedimentation of dissolved and suspended matter during different river discharge rates, Mar. Geol., 222, 135–158, 2005.

Correggiari, A., Cattaneo, A., and Trincardi, F.: The modern Po Delta system: Lobe switching and asymmetric prodelta growth, Mar. Geol., 222, 49–74, 2005.

Fox, J. M., Hill, P. S., Milligan, T. G., and Boldrin, A.: Flocculation and sedimentation on the Po River Delta, Mar. Geol., 203, 95–107, 2004.

Frignani, M., Langone, L., Ravaioli, M., Sorgente, D., Alvisi, F., and Albertazzi, S.: Fine-

BGD

7, 7849–7902, 2010

sediment mass balance in the western Adriatic continental shelf over a century time scale, Mar. Geol., 222, 113–133, 2005.
Fry, B. and Sherr, E. B.: Delta-C-13 Measurements as Indicators of Carbon Flow in Marine and Fresh-Water Ecosystems, Contrib. Mar. Sci., 27, 13–47, 1984.
Giani, M., Berto, D., Rampazzo, F., Savelli, F., Alvisi, F., Giordano, P., Ravaioli, M., and Frascari, F.: Origin of sedimentary organic matter in the north-western Adriatic Sea, Estuar. Coast. Shelf S., 84, 573–583, 2009.
Gomez, B., Trustrum, N. A., Hicks, D. M., Rogers, K. M., Page, M. J., and Tate, K. R.: Production, storage, and output of particulate organic carbon: Waipaoa River basin, New Zealand, Water Resour. Res., 39, 1161, doi:10.1029/2002WR001619, 2003.
Goni, M. A., Ruttenberg, K. C., and Eglinton, T. I.: A reassessment of the sources and importance of land-derived organic matter in surface sediments from the Gulf of Mexico, Geochim. Cosmochim. Ac., 62, 3055–3075, 1998.
Goni, M. A., Teixeira, M. J., and Perkey, D. W.: Sources and distribution of organic matter in a river-dominated estuary (Winyah Bay, SC, USA), Estuar. Coast. Shelf S., 57, 1023–1048, 2003.
Goni, M. A., Yunker, M. B., Macdonald, R. W., and Eglinton, T. I.: The supply and preservation of ancient and modem components of organic carbon in the Canadian Beaufort Shelf of the Arctic Ocean, Mar. Chem., 93, 53–73, 2005.
Goni, M. A., Monacci, N., Gisewhite, R., Crockett, J., Nittrouer, C., Ogston, A., Alin, S. R., and Aalto, R.: Terrigenous organic matter in sediments from the Fly River delta-clinoform system (Papua New Guinea), J. Geophys. Res.-Earth, 113, F01S10, doi:10.1029/2006JF000653, 2008.
Gordon, E. S. and Goni, M. A.: Sources and distribution of terrigenous organic matter delivered by the Atchafalaya River to sediments in the northern Gulf of Mexico, Geochim. Cosmochim. Ac., 67, 2359–2375, 2003.
Harmelin-Vivien, M., Loizeau, V., Mellon, C., Beker, B., Arlhac, D., Bodiguel, X., Ferraton, F., Hermand, R., Philippon, X., and Salen-Picard, C.: Comparison of C and N stable isotope ratios between surface particulate organic matter and microphytoplankton in the Gulf of Lions (NW Mediterranean), Cont. Shelf Res., 28, 1911–1919, 2008.
Hedges, J. I. and Mann, D. C.: Characterization of Plant-Tissues by Their Lignin Oxidation-Products, Geochim. Cosmochim. Ac., 43, 1803–1807, 1979.
Hedges, J. I., Clark, W. A., Quay, P. D., Richey, J. E., Devol, A. H., and Santos, U. D.: Compo-

BGD
7, 7849–7902, 2010

sitions and Fluxes of Particulate Organic Material in the Amazon River, Limnol. Oceanogr., 31, 717–738, 1986.
Hedges, J. I. and Keil, R. G.: Sedimentary Organic-Matter Preservation – an Assessment and Speculative Synthesis, Mar. Chem., 49, 81–115, 1995.
Hedges, J. I. and Oades, J. M.: Comparative organic geochemistries of soils and marine sediments, Org. Geochem., 27, 319–361, 1997.
Hernes, P. J., Robinson, A. C., and Aufdenkampe, A. K.: Fractionation of lignin during leaching and sorption and implications for organic matter "freshness", Geophys. Res. Lett., 34, L17401, doi:10.1029/2007GL031017, 2007.
Hinga, K. R., Arthur, M. A., Pilson, M. E. Q., and Whitaker, D.: Carbon-Isotope Fractionation by Marine-Phytoplankton in Culture – the Effects of Co_2 Concentration, Ph, Temperature, and Species, Global Biogeochem. Cy., 8, 91–102, 1994.
Kettner, A. J. and Syvitski, J. P. M.: Fluvial responses to environmental perturbations in the Northern Mediterranean since the Last Glacial Maximum, Quaternary Sci. Rev., 28, 2386–2397, 2009.
Leithold, E. L., Blair, N. E., and Perkey, D. W.: Geomorphologic controls on the age of particulate organic carbon from small mountainous and upland rivers, Global Biogeochem. Cy., 20, GB3022, doi:10.1029/2005GB002677, 2006.
Mayer, L. M.: Surface-Area Control of Organic-Carbon Accumulation in Continental-Shelf Sediments, Geochim. Cosmochim. Ac., 58, 1271–1284, 1994.
Milligan, T. G., Hill, P. S., and Law, B. A.: Flocculation and the loss of sediment from the Po River plume, Cont. Shelf Res., 27, 309–321, 2007.
Milliman, J. D. and Syvitski, J. P. M.: Geomorphic Tectonic Control of Sediment Discharge to the Ocean – the Importance of Small Mountainous Rivers, J. Geol., 100, 525–544, 1992.
Miserocchi, S., Langone, L., and Tesi, T.: Content and isotopic composition of organic carbon within a flood layer in the Po River prodelta (Adriatic Sea), Cont. Shelf Res., 27, 338–358, 2007.
Mortlock, R. A. and Froelich, P. N.: A Simple Method for the Rapid-Determination of Biogenic Opal in Pelagic Marine-Sediments, Deep-Sea Res. Pt. I, 36, 1415–1426, 1989.
Onstad, G. D., Canfield, D. E., Quay, P. D., and Hedges, J. I.: Sources of particulate organic matter in rivers from the continental USA: Lignin phenol and stable carbon isotope compositions, Geochim. Cosmochim. Ac., 64, 3539–3546, 2000.
Opsahl, S. and Benner, R.: Early Diagenesis of Vascular Plant-Tissues – Lignin and Cutin De-

BGD
7, 7849–7902, 2010

composition and Biogeochemical Implications, Geochim. Cosmochim. Ac., 59, 4889–4904, 1995.
Palinkas, C. M., Nittrouer, C. A., Wheatcroft, R. A., and Langone, L.: The use of Be-7 to identify event and seasonal sedimentation near the Po River delta, Adriatic Sea, Mar. Geol., 222, 95–112, 2005.
Svendsen, K. M., Renshaw, C. E., Magilligan, F. J., Nislow, K. H., and Kaste, J. M.: Flow and sediment regimes at tributary junctions on a regulated river: impact on sediment residence time and benthic macroinvertebrate communities, Hydrol. Process., 23, 284–296, 2009.
Syvitski, J. P. M., Kettner, A. J., Correggiari, A., and Nelson, B. W.: Distributary channels and their impact on sediment dispersal, Mar. Geol., 222, 75–94, 2005a.
Syvitski, J. P. M., Vorosmarty, C. J., Kettner, A. J., and Green, P.: Impact of humans on the flux of terrestrial sediment to the global coastal ocean, Science, 308, 376–380, 2005b.
Syvitski, J. P. M. and Kettner, A. J.: On the flux of water and sediment into the Northern Adriatic Sea, Cont. Shelf Res., 27, 296–308, 2007.
Syvitski, J. P. M., Kettner, A. J., Overeem, I., Hutton, E. W. H., Hannon, M. T., Brakenridge, G. R., Day, J., Vorosmarty, C., Saito, Y., Giosan, L., and Nicholls, R. J.: Sinking deltas due to human activities, Nat. Geosci., 2, 681–686, 2009.
Tesi, T., Miserocchi, S., Goni, M. A., and Langone, L.: Source, transport and fate of terrestrial organic carbon on the western Mediterranean Sea, Gulf of Lions, France, Mar. Chem., 105, 101–117, 2007.
Tesi, T., Langone, L., Goni, M. A., Miserocchi, S., and Bertasi, F.: Changes in the composition of organic matter from prodeltaic sediments after a large flood event (Po River, Italy), Geochim. Cosmochim. Ac., 72, 2100–2114, 2008.
Traykovski, P., Wiberg, P. L., and Geyer, W. R.: Observations and modeling of wave-supported sediment gravity flows on the Po prodelta and comparison to prior observations from the Eel shelf, Cont. Shelf Res., 27, 375–399, 2007.
Wheatcroft, R. A., Stevens, A. W., Hunt, L. M., and Milligan, T. G.: The large-scale distribution and internal geometry of the fall 2000 Po River flood deposit: Evidence from digital X-radiography, Cont. Shelf Res., 26, 499–516, 2006.
Wheatcroft, R. A., Goni, M. A., Hatten, J. A., Pasternack, G. B., and Warrick, J. A.: The role of effective discharge in the ocean delivery of particulate organic carbon by small, mountainous river systems, Limnol. Oceanogr., 55, 161–171, 2010.

BGD
7, 7849–7902, 2010

Table 1. Po river samples collected at Pontelagoscuro (PLS).

Sample		SSC	OC	TN	OC	TN	$\delta^{13}C$	$\Delta^{14}C$	OC:TN
		[mg/l]	[wt%]		[µg/l]		[‰]		[ratio]
PLS right	coarse, >63 µm	8.8	3.6	0.26	316.9	23.1	−27.1		13.7
PLS center	coarse, >63 µm	8.7	4.2	0.31	365.6	26.7	−27.0	−46.1	13.7
PLS left	coarse, >63 µm	4.2	4.8	0.35	203.8	14.9	−27.1		13.7
	average	*7.2*	*4.2*	*0.31*	*295.4*	*21.6*	*−27.1*		*13.7*
	s.d.	*2.6*	*0.6*	*0.04*	*83.0*	*6.1*	*0.1*		*0.0*
PLS right	fine, <63 µm	439.2	1.3	0.14	5501.8	633.0	−26.0		8.7
PLS center	fine, <63 µm	465.4	1.1	0.15	5280.6	687.4	−25.6	−241	7.7
PLS left	fine, <63 µm	417.9	1.1	0.14	4738.5	601.4	−25.7		7.9
	average	*440.8*	*1.2*	*0.15*	*5173.6*	*640.6*	*−25.8*		*8.1*
	s.d.	*23.8*	*0.1*	*0.01*	*392.7*	*43.5*	*0.2*		*0.5*

BGD
7, 7849–7902, 2010

Table 2. Lignin biomarkers of Po river samples collected at Pontelagoscuro (PLS).

Sample		S	V	C	Λ	C:V	S:V	Vd:Vl	Sd:Sl
		[mg/100 mg OCl]							
PLS right	coarse, >63 µm	2.75	2.58	0.70	6.02	0.27	1.07	0.55	0.52
PLS center	coarse, >63 µm	2.69	2.89	0.71	6.29	0.25	0.93	0.58	0.53
PLS left	coarse, >63 µm	2.52	2.44	0.32	5.29	0.13	1.03	0.60	0.57
	average	*2.65*	*2.64*	*0.58*	*5.87*	*0.22*	*1.01*	*0.58*	*0.54*
	s.d.	*0.12*	*0.23*	*0.22*	*0.52*	*0.07*	*0.07*	*0.03*	*0.03*
PLS right	fine, <63 µm	0.69	0.63	0.20	1.51	0.31	1.10	0.76	0.67
PLS center	fine, <63 µm	0.72	0.70	0.26	1.68	0.38	1.03	1.27	1.23
PLS left	fine, <63 µm	0.83	0.68	0.26	1.77	0.38	1.23	1.10	0.78
	average	*0.75*	*0.67*	*0.24*	*1.66*	*0.36*	*1.12*	*1.05*	*0.89*
	s.d.	*0.07*	*0.04*	*0.04*	*0.13*	*0.04*	*0.10*	*0.26*	*0.30*

BGD
7, 7849–7902, 2010

Table 3. Physical parameters for suspended sediment samples collected in the Po prodelta before and during the peak discharge.

Discharge	Level	Channel	Location	Salinity	Transittance	Fluorescence	SSC	D_{50}
				[PSU]	[%]	[a.u.]	[mg/l]	[um]
Moderate	Top	Pila	North	31.9 ± 0.9	41.0 ± 13.3	0.67 ± 0.16	5.0 ± 2.9	5.8 ± 1.3
		Tolle	Center	29.9 ± 3.1	51.8 ± 13.3	0.66 ± 0.30	2.7 ± 1.4	6.0 ± 0.4
		Goro/Gnocca	South	27.6 ± 1.1	51.7 ± 6.14	0.73 ± 0.11	2.9 ± 0.3	5.6 ± 1.3
			average top	*29.8 ± 2.5*	*47.7 ± 11.6*	*0.69 ± 0.18*	*3.8 ± 2.2*	*5.8 ± 1.1*
	Bottom	Pila	North	35.6 ± 1.3	43.7 ± 28.6	0.29 ± 0.16	4.6 ± 2.1	4.8 ± 1.2
		Tolle	Center	36.7 ± 1.1	12.2 ± 18.9	0.21 ± 0.04	7.6 ± 4.1	4.0 ± 0.8
		Goro/Gnocca	South	37.5 ± 0.2	21.1 ± 24.1	0.21 ± 0.03	6.0 ± 2.9	3.7 ± 0.3
			average bottom	*36.5 ± 1.3*	*28.7 ± 27.4*	*0.25 ± 0.11*	*5.5 ± 3.4*	*4.3 ± 1.0*
Peak	Top	Pila	North	25.6 ± 0.8	27.4 ± 24.4	0.64 ± 0.10	24.4 ± 26.5	6.3 ± 2.3
		Tolle	Center	17.5 ± 4.5	12.0 ± 13.1	0.73 ± 0.57	13.5 ± 11.1	4.9 ± 0.3
		Goro/Gnocca	South	21.3 ± 2.6	29.7 ± 8.18	1.25 ± 0.58	5.6 ± 0.1	5.2 ± 0.6
			average top	*21.5 ± 4.5*	*22.5 ± 17.7*	*0.84 ± 0.49*	*15.5 ± 18.1*	*5.6 ± 1.5*
	Bottom	Pila	North	35.8 ± 2.1	46.5 ± 33.5	0.14 ± 0.02	7.8 ± 9.5	5.4 ± 2.0
		Tolle	Center	36.1 ± 1.8	51.1 ± 17.9	0.13 ± 0.04	5.5 ± 3.6	4.8 ± 1.6
		Goro/Gnocca	South	36.8 ± 1.1	44.8 ± 13.1	0.14 ± 0.04	3.4 ± 1.3	3.8 ± 0.5
			average bottom	*36.2 ± 1.6*	*47.7 ± 21.8*	*0.14 ± 0.03*	*5.3 ± 7.0*	*4.7 ± 1.5*

BGD
7, 7849–7902, 2010

Table 4. Bulk composition for suspended sediment samples collected in the Po prodelta before and during the peak discharge.

Discharge	Level	Channel	Location	OC	TN	OC	TN	δ^{13}C	OC:TN
				[wt%]		[µg/l]		[‰]	[ratio]
Moderate	Top	Pila	North	6.1 ± 2.9	1.08 ± 0.52	200 ± 33	36 ± 6	−23.8 ± 0.5	5.6 ± 0.2
		Tolle	Center	1.5 ± 0.6	1.46 ± 0.6	229 ± 51	42 ± 10	−24.6 ± 1.2	5.4 ± 0.1
		Goro/Gnocca	South	1.4 ± 0.5	1.36 ± 0.53	202 ± 50	37 ± 10	−24.9 ± 0.4	5.4 ± 0.1
			average top	*6.9 ± 2.8*	*1.26 ± 0.53*	*208 ± 43*	*38 ± 9*	*−24.3 ± 0.8*	*5.5 ± 0.2*
	Bottom	Pila	North	0.9 ± 0.4	0.92 ± 0.41	188 ± 43	31 ± 6	−23.8 ± 0.5	5.7 ± 0.3
		Tolle	Center	2.9 ± 1.6	0.54 ± 0.32	171 ± 54	31 ± 9	−24.3 ± 0.6	5.4 ± 0.3
		Goro/Gnocca	South	3.4 ± 2.6	0.63 ± 0.48	141 ± 13	25 ± 2	−24.3 ± 0.4	5.5 ± 0.2
			average bottom	*4.1 ± 2.4*	*0.73 ± 0.42*	*169 ± 43*	*30 ± 6*	*−24.1 ± 0.5*	*5.6 ± 0.3*
Peak	Top	Pila	North	5.1 ± 4.2	0.9 ± 0.8	521 ± 461	83 ± 68	−24.6 ± 1.1	6.1 ± 0.9
		Tolle	Center	3.2 ± 1.3	0.59 ± 0.27	329 ± 105	58 ± 14	−24.9 ± 0.5	5.5 ± 0.4
		Goro/Gnocca	South	5.8 ± 2.1	1.1 ± 0.35	328 ± 123	61 ± 20	−25.5 ± 1.3	5.3 ± 0.2
			average top	*4.7 ± 2.9*	*0.87 ± 0.55*	*406 ± 295*	*70 ± 43*	*−25 ± 1*	*5.7 ± 0.7*
	Bottom	Pila	North	5.5 ± 2.9	0.99 ± 0.57	201 ± 182	31 ± 23	−23.9 ± 1	5.9 ± 0.9
		Tolle	Center	4.4 ± 1.3	0.75 ± 0.36	165 ± 111	24 ± 11	−24.3 ± 0.8	6.3 ± 1.6
		Goro/Gnocca	South	3.9 ± 0.5	0.82 ± 0.14	106 ± 29	22 ± 8	−24.1 ± 0.4	4.8 ± 0.5
			average bottom	*4.7 ± 2*	*0.87 ± 0.39*	*162 ± 126*	*27 ± 15*	*−24.1 ± 0.8*	*5.7 ± 1.1*

BGD
7, 7849–7902, 2010

Table 5. Lignin biomarkers for suspended sediment samples collected in the Po prodelta before and during the peak discharge.

Discharge	Level	Channel	Location	S	V	C	Λ	C:V	S:V	Vd:Vl	Sd:Sl
				[mg/100 mg OC]							
Moderate	Top	Pila	North	0.23 ± 0.08	0.19 ± 0.08	0.06 ± 0.05	0.48 ± 0.18	0.40 ± 0.09	1.24 ± 0.24	1.13 ± 0.26	0.97 ± 0.3
		Tolle	Center	0.08 ± 0.04	0.08 ± 0.03	0.04 ± 0.03	0.2 ± 0.07	0.73 ± 0.28	1.13 ± 0.4	0.69 ± 0.12	0.76 ± 0.14
		Goro/Gnocca	South	0.11 ± 0.04	0.08 ± 0.05	0.06 ± 0.01	0.23 ± 0.1	0.77 ± 0.09	1.33 ± 0.16	0.92 ± 0.14	0.95 ± 0.07
			average top	*0.15 ± 0.09*	*0.12 ± 0.08*	*0.05 ± 0.04*	*0.32 ± 0.18*	*0.59 ± 0.23*	*1.24 ± 0.26*	*0.94 ± 0.26*	*0.92 ± 0.21*
	Bottom	Pila	North	0.27 ± 0.12	0.28 ± 0.07	0.1 ± 0.03	0.58 ± 0.18	0.44 ± 0.13	0.97 ± 0.42	0.8 ± 0.12	0.74 ± 0.05
		Tolle	Center	0.26 ± 0.08	0.16 ± 0.05	0.1 ± 0.05	0.51 ± 0.17	0.63 ± 0.16	1.67 ± 0.24	0.81 ± 0.11	0.7 ± 0.08
		Goro/Gnocca	South								
			average bottom	*0.26 ± 0.09*	*0.22 ± 0.09*	*0.1 ± 0.04*	*0.55 ± 0.16*	*0.58 ± 0.16*	*1.32 ± 0.49*	*0.8 ± 0.1*	*0.72 ± 0.07*
Peak	Top	Pila	North	0.58 ± 0.27	0.51 ± 0.2	0.15 ± 0.06	1.23 ± 0.53	0.29 ± 0	1.12 ± 0.08	1 ± 0.26	0.79 ± 0.27
		Tolle	Center	0.24 ± 0.13	0.29 ± 0.17	0.04 ± 0.01	0.56 ± 0.31	0.15 ± 0.05	0.85 ± 0.07	1.97 ± 0.36	1.63 ± 0.42
		Goro/Gnocca	South	0.12 ± 0.02	0.1 ± 0.04	0.05 ± 0.02	0.27 ± 0.05	0.51 ± 0.29	1.18 ± 0.2	1.26 ± 0.28	1.2 ± 0.31
			average top	*0.28 ± 0.24*	*0.27 ± 0.21*	*0.07 ± 0.06*	*0.63 ± 0.5*	*0.34 ± 0.24*	*1.07 ± 0.2*	*1.39 ± 0.48*	*1.21 ± 0.44*

BGD
7, 7849–7902, 2010

Table 6. Penetration of ^{7}Be for sediment core samples collected in the Po prodelta before and after the peak discharge. ^{7}Be penetrations for the October 2000 flood were shown as comparison.

Collection date	Station	Distributary channel	Depth	Lat	Long	^{7}Be penetration	Oct-2000 flood thickness*
			[m]	[° N]	[° E]	[cm]	[cm]
Before the peak							
30-Apr-09	E11	Pila	12.0	44.970	12.575	10	~36
30-Apr-09	E16	Pila	20.8	44.974	12.575	5	~36
30-Apr-09	E20	Pila	15.0	44.975	12.582	1	~36
30-Apr-09	H18	Pila	17.0	44.916	12.582	0	~5
30-Apr-09	J13	Tolle	13.8	44.868	12.520	1	~25
30-Apr-09	J20	Tolle	20.5	44.858	12.553	2	~12
30-Apr-09	N14	Goro/Gnocca	12.0	44.796	12.462	0	~12
1-May-09	G10	Pila	11.2	44.946	12.572	1	~8
1-May-09	G15	Pila	15.9	44.942	12.589	2	~5
1-May-09	H10	Pila	11.6	44.923	12.556	0	~12
After the peak							
5-May-09	E16-II	Pila	16.3	44.974	12.576	17	~36
5-May-09	J13-II	Tolle	14.1	44.868	12.521	5	~25

*from Wheatcroft et al. (2006)

BGD
7, 7849–7902, 2010

Table 7. Bulk compositions for sediment cores collected in the Po prodelta. See Fig. 1 for core location.

		Interval	OC	TN	$\delta^{13}C$	$\Delta^{14}C$	OC:TN	SA	D_{50}
		[cm]	[wt%]		[‰]		[ratio]	[m^2/g]	[μm]
North – Core E16II – Flood deposit	*North Core E16.II*								
		0–1	1.3	0.14	−27.0	−204.8	8.69	13.2	n.a.
		1–2	1.3	0.15	−26.9		8.51	13.9	n.a.
		2–3	1.2	0.16	−27.0		7.86	10.0	10.5
		3–4	1.0	0.12	−26.7		8.52	15.2	15.4
		4–5	1.2	0.14	−26.9		8.84	14.9	9.0
		5–6	0.9	0.10	−26.9	−176.7	8.59	12.8	10.6
		6–7	1.2	0.13	−27.1		8.99	14.5	7.4
		7–8	1.1	0.13	−26.7		8.55	12.7	9.7
		8–9	1.2	0.14	−26.9	−193.7	8.63	11.6	7.4
		9–10	1.2	0.15	−26.4		7.82	15.3	4.1
		10–11	1.1	0.13	−26.7		8.47	13.4	6.5
		11–12	1.2	0.12	−26.9		9.50	15.7	7.0
		12–13	1.2	0.15	−26.6		8.08	15.9	4.7
		13–14	0.9	0.12	−26.3	−222.3	7.57	14.8	4.7
		14–15	0.5	0.07	−26.1		7.87	5.3	23.7
		15–16	0.4	0.05	−25.6		7.02	4.5	29.4
		16–17	0.5	0.07	−25.8	−339.4	7.35	5.0	23.5
	average		*1.0*	*0.12*	*−26.6*	*−227.4*	*9.7*	*12.3*	*11.6*
	s.d.		*0.3*	*0.03*	*0.4*	*64.8*	*0.7*	*3.8*	*7.9*
Flood deposit	*Center Core J13.II*								
		0–0.5	1.2	0.15	−26.3	−204.1	7.63	27.1	2.0
		0.5–1	1.3	0.16	−26.3		7.75	26.7	1.7
		1–2	1.5	0.18	−26.4	−205.5	8.16	28.9	1.7
		2–3	1.0	0.13	−26.2		7.83	20.6	2.9
		3–4	1.3	0.15	−26.1	−207.6	8.32	22.0	2.0
		4–5	0.8	0.10	−24.6		8.09	20.7	7.6
		5–6	0.3	0.04	−24.2	−312.0	7.28	15.0	11.7
	average		*1.0*	*0.13*	*−25.7*	*−232.3*	*9.2*	*23.0*	*4.2*
	s.d.		*0.4*	*0.05*	*0.9*	*53.2*	*0.4*	*4.9*	*3.9*
Bioturbated deposit	*South Core N14*								
		0–1	0.61	0.09	−24.85		6.7	14.92	n.a.
		1–2	0.70	0.08	−25.23		8.5	18.35	n.a.
		2–3	0.69	0.08	−25.29		8.3	23.30	n.a.
		3–4	0.79	0.09	−25.33		8.3	21.25	n.a.
		4–5	0.76	0.09	−25.46		8.5	14.54	n.a.
		5–6	0.51	0.06	−25.01		8.0	15.64	n.a.
		6–7	0.40	0.05	−24.94		7.8	20.54	n.a.
		7–8	0.46	0.06	−25.1		7.7	14.80	n.a.
		8–9	0.63	0.08	−25.38		8.0	n.a.	n.a.
		9–10	0.55	0.07	−25.47		7.4	16.52	n.a.
		10–11	0.71	0.09	−25.68		8.1	n.a.	n.a.
		11–12	0.54	0.07	−25.44		7.7	n.a.	n.a.
		12–13	0.63	0.08	−25.78		7.5	22.73	n.a.
		13–14	0.63	0.08	−25.59		7.8	27.68	n.a.
		14–15	0.70	0.09	−25.58		8.0	17.26	n.a.
		15–16	0.56	0.07	−25.55		7.6	16.01	n.a.
		16–17	0.63	0.08	−25.59		8.1	15.09	n.a.
	average		*0.6*	*0.08*	*−25.4*		*7.9*	*18.5*	
	s.d.		*0.1*	*0.01*	*0.3*		*0.4*	*4.0*	

n.a. = not avaliable

BGD
7, 7849–7902, 2010

Table 8. Lignin biomarkers for sediment cores collected in the Po prodelta after the May 2009 flood.

	Interval	S	V	C	Λ	C:V	S:V	Vd:Vl	Sd:Sl
	[cm]	[mg/100 mg OC]							
North Core E16_II									
Flood deposit	0–1	1.25	1.22	0.38	2.85	0.31	1.03	0.35	0.37
	1–2	1.36	1.31	0.39	3.06	0.30	1.04	0.41	0.40
	2–3	1.39	1.32	0.40	3.12	0.30	1.05	0.39	0.40
	3–4	1.66	1.59	0.48	3.73	0.30	1.05	0.35	0.34
	4–5	1.41	1.37	0.40	3.19	0.29	1.03	0.49	0.50
	5–6	2.04	1.96	0.58	4.58	0.29	1.04	0.38	0.39
	6–7	1.24	1.27	0.33	2.85	0.26	0.98	0.49	0.53
	7–8	1.38	1.45	0.40	3.23	0.28	0.96	0.35	0.39
	8–9	1.27	1.15	0.37	2.79	0.32	1.10	0.38	0.36
	9–10	1.08	1.08	0.31	2.47	0.29	1.01	0.40	0.44
	10–11	1.46	1.48	0.41	3.36	0.28	0.98	0.40	0.43
	11–12	1.24	1.25	0.37	2.86	0.29	0.99	0.34	0.35
	12–13	0.97	0.91	0.29	2.17	0.32	1.07	0.39	0.37
	13–14	1.05	0.89	0.32	2.26	0.36	1.18	0.43	0.40
	14–15	1.11	1.11	0.37	2.59	0.34	1.00	0.49	0.51
	15–16	1.38	1.32	0.53	3.23	0.40	1.05	0.50	0.47
	16–17	1.53	1.38	0.59	3.50	0.43	1.11	0.46	0.41
average		*1.34*	*1.30*	*0.41*	*3.05*	*0.32*	*1.04*	*0.41*	*0.42*
s.d.		*0.25*	*0.25*	*0.09*	*0.58*	*0.04*	*0.06*	*0.05*	*0.06*
Center Core J13_II									
Flood deposit	0–0.5	0.81	0.77	0.23	1.81	0.30	1.05	0.49	0.49
	0.5–1	1.08	0.97	0.30	2.35	0.31	1.12	0.48	0.47
	1–2	1.09	0.99	0.32	2.39	0.32	1.10	0.44	0.40
	2–3	0.92	0.82	0.29	2.03	0.35	1.13	0.47	0.44
	3–4	0.87	0.78	0.28	1.94	0.36	1.12	0.39	0.35
	4–5	0.74	0.75	0.26	1.75	0.35	0.99	0.46	0.45
	5–6	0.85	0.69	0.43	1.98	0.62	1.23	0.45	0.48
average		*0.91*	*0.82*	*0.30*	*2.03*	*0.37*	*1.11*	*0.45*	*0.44*
s.d.		*0.13*	*0.11*	*0.06*	*0.25*	*0.11*	*0.07*	*0.03*	*0.05*

BGD
7, 7849–7902, 2010

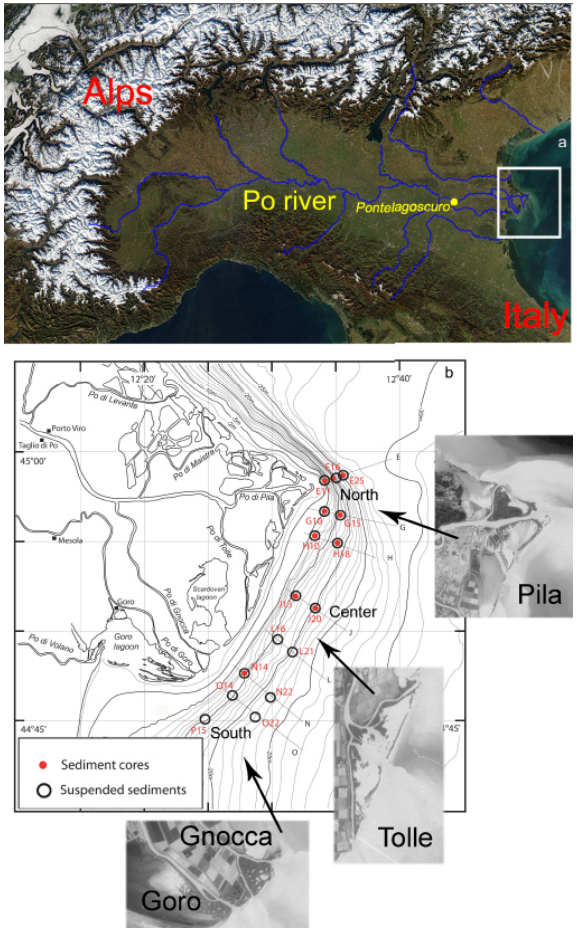

Fig. 1. (a) Satellite image of the Northern Italy and Po river drainage basin. The open square shows the Po prodelta location **(b)** Map of the study area. Stations were grouped in the sub-regions: north, center, and south.

BGD
7, 7849–7902, 2010

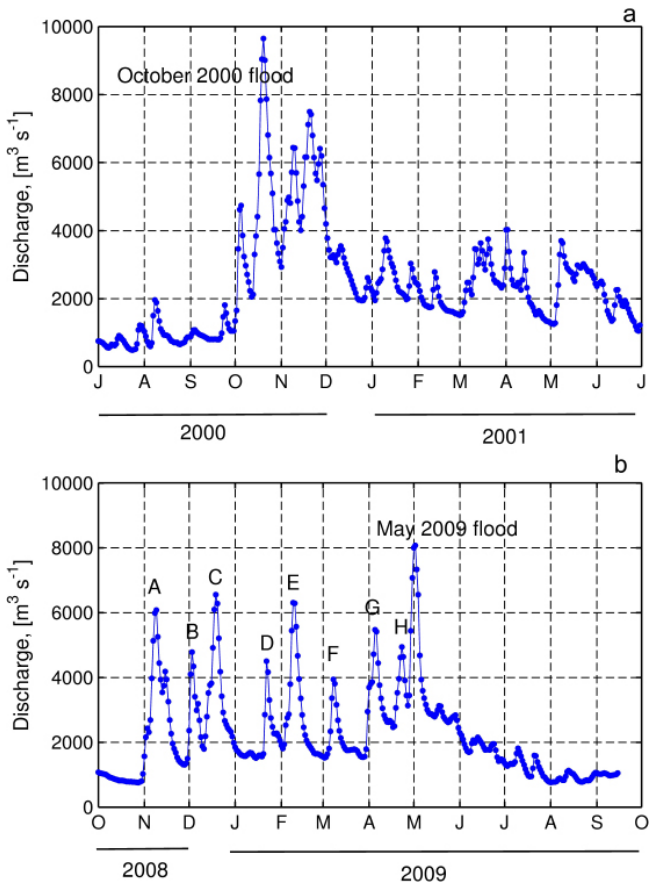

Fig. 2. **(a)** Po river discharge at Pontelagoscuro station from June 2000 through July 2001. **(b)** 1-year Po river discharge at Pontelagoscuro station from October 2008 through October 2009.

BGD
7, 7849–7902, 2010

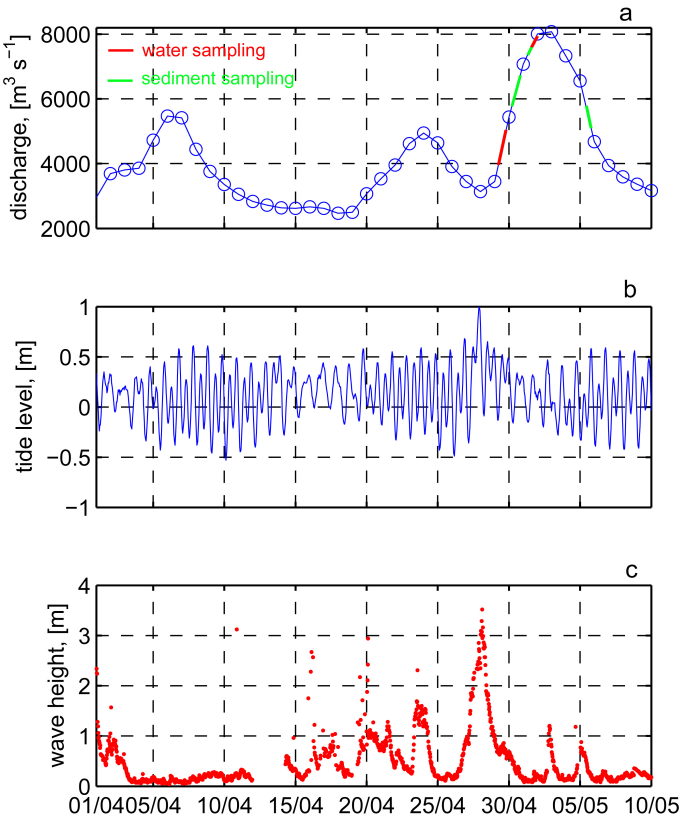

Fig. 3. Time-series data from 1 April through 10 May. **(a)** River discharge during sampling in the prodelta. **(b)** Tide level. **(c)** Wave height.

BGD
7, 7849–7902, 2010

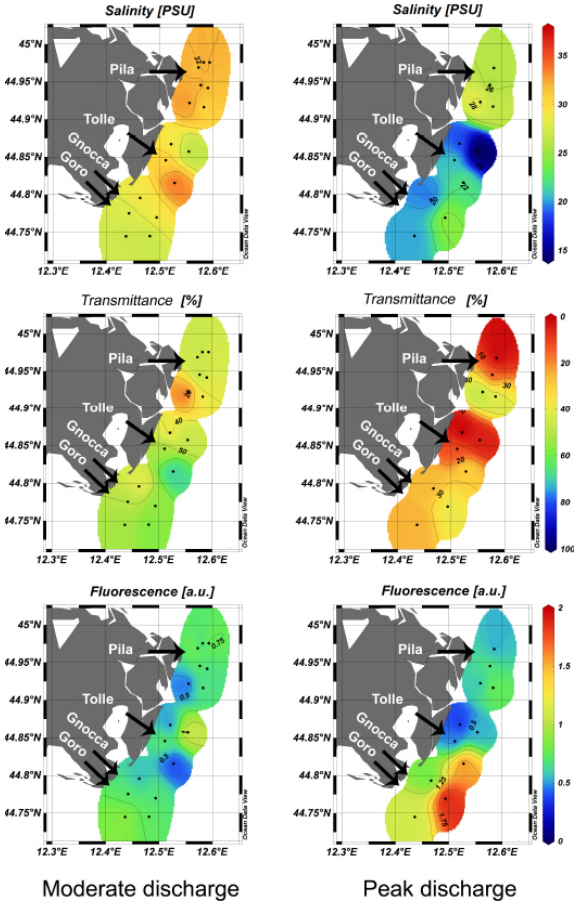

Fig. 4. Salinity, transmittance, and fluorescence in the Po prodelta in surface waters (1 m below the sea surface) during moderate (~5000 $m^3 s^{-1}$) and peak discharge (~8000 $m^3 s^{-1}$).

BGD
7, 7849–7902, 2010

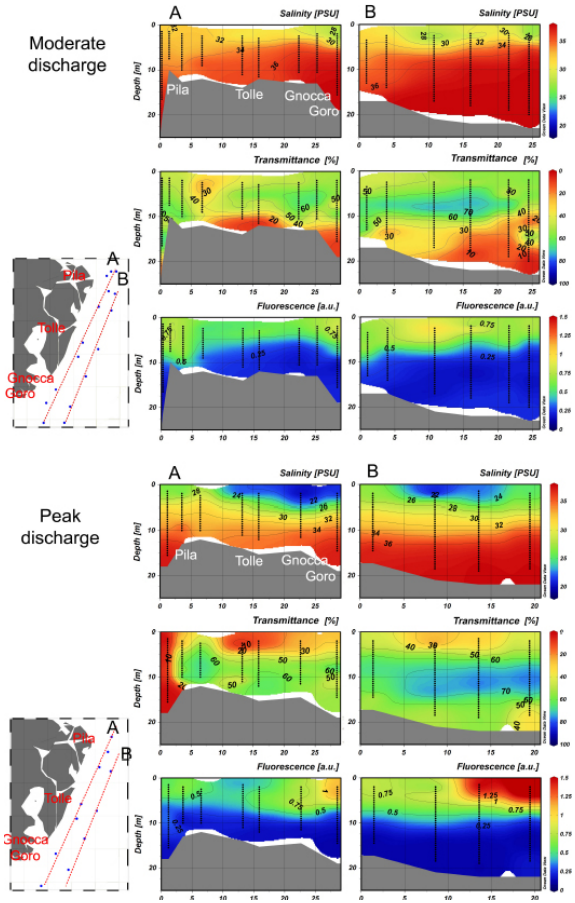

Fig. 5. Salinity, transmittance, and fluorescence in the Po prodelta along two shore-parallel sections during moderate (~5000 $m^3 s^{-1}$) and peak discharge (~8000 $m^3 s^{-1}$).

BGD
7, 7849–7902, 2010

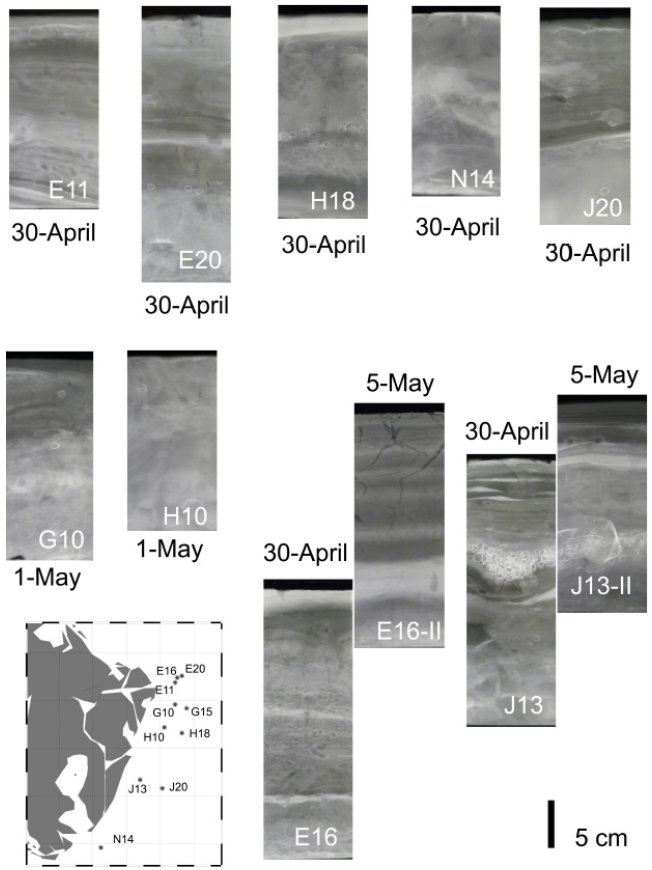

Fig. 6. Radiographs of sediment cores collected in Po prodelta in 30 April, 1 May, and 5 May.

BGD
7, 7849–7902, 2010

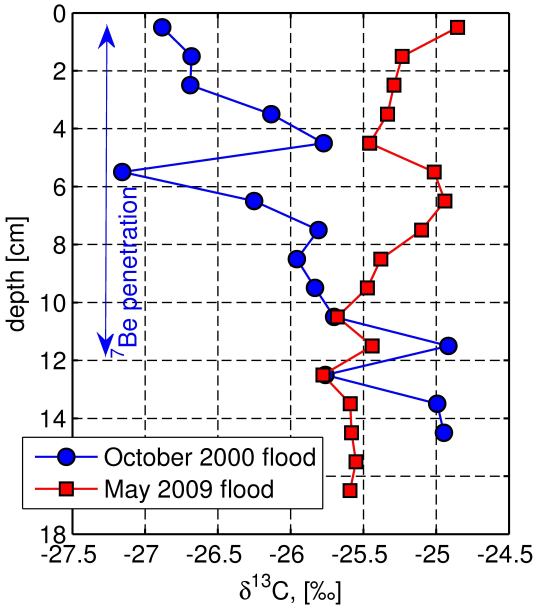

Fig. 7. Down-core profiles of $\delta^{13}C$. Filled circles show the N14 core collected in December 2000 (Miserocchi et al., 2007). Solid line shows the ^{7}Be penetration (Palinkas et al., 2008). Filled squares show the N14 core collected on 30 April 2009.

BGD
7, 7849–7902, 2010

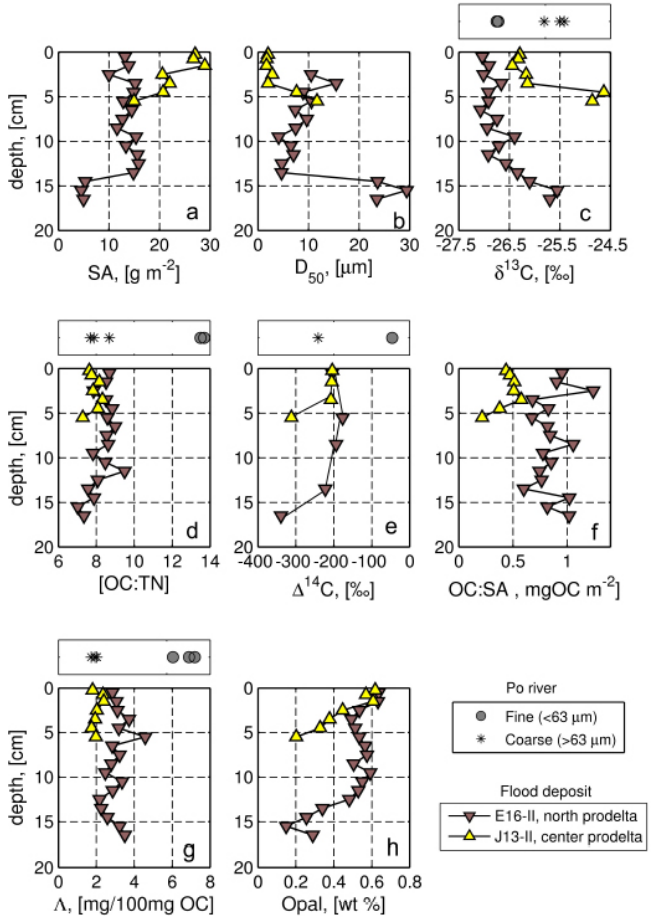

Fig. 8. Down-core variability in flood deposits collected in the north (E16-II) and central (J13-II) prodelta vs. material collected in the Po river: **(a)** SA, **(b)** D_{50}, **(c)** δ^{13}C, **(d)** OC:TN, **(e)** Δ^{14}C, **(f)** OC:SA, **(g)** Λ, and **(h)** Opal.

BGD
7, 7849–7902, 2010

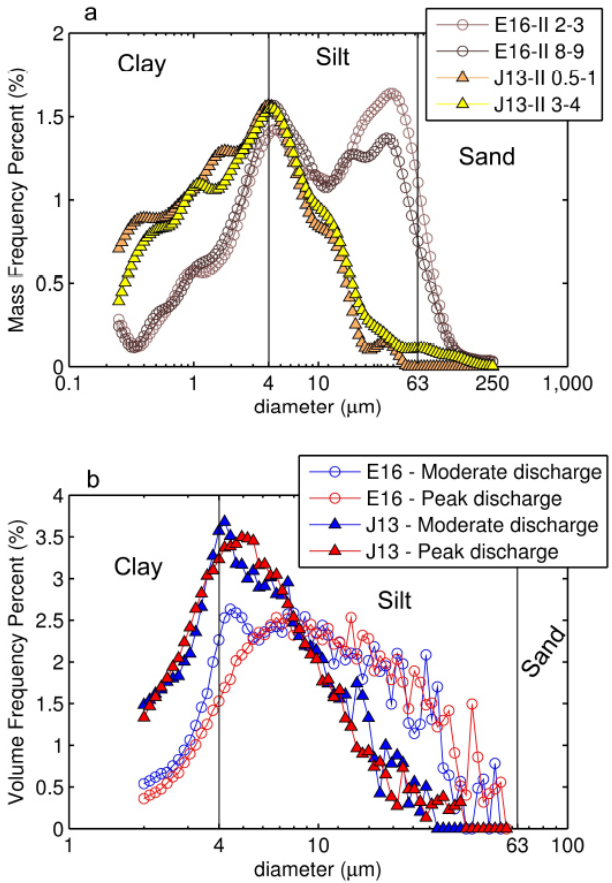

Fig. 9. (a) Grain-size distribution of E16-II and J13-II sediment core. Two intervals are shown for each core (Sedigrapher). **(b)** Grain-size distribution of surface suspended sediments at E16 and J13 stations (Coulter Counter).

BGD
7, 7849–7902, 2010

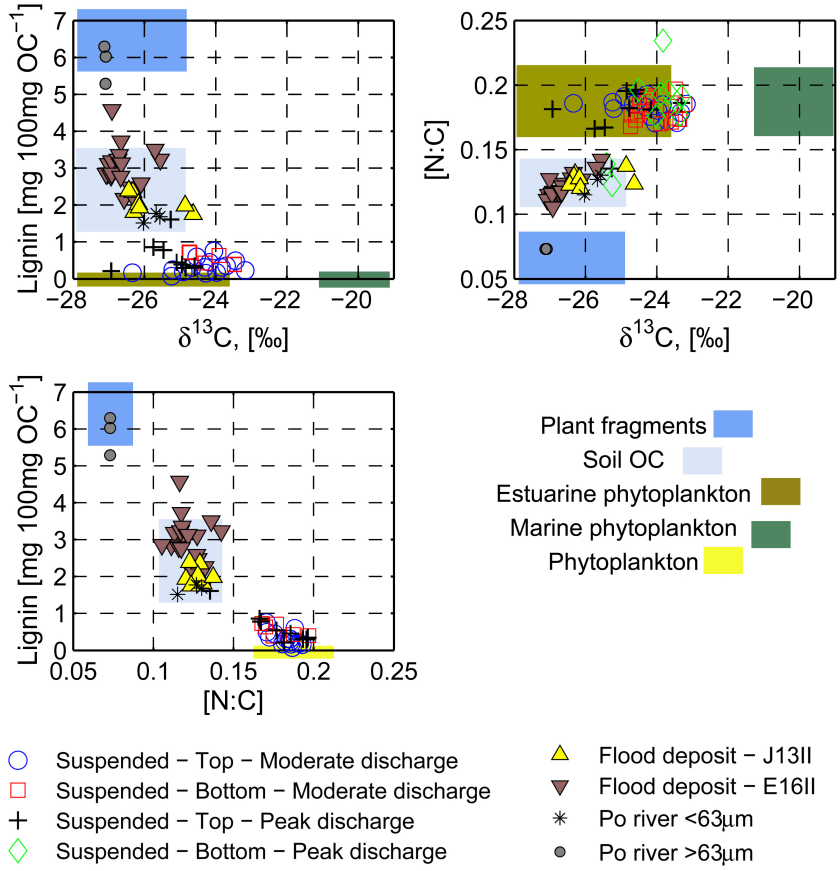

Fig. 10. Sources of OC in Po river samples, suspended materials and flood deposits collected in the Po prodelta. Boxes show the relative contribution of allochthonous and autochthonous OC according to the average values in literature (Fry and Sherr, 1984; Hedges et al., 1986; Goni et al., 2003; Harmelin-Vivien et al., 2008).

BGD
7, 7849–7902, 2010

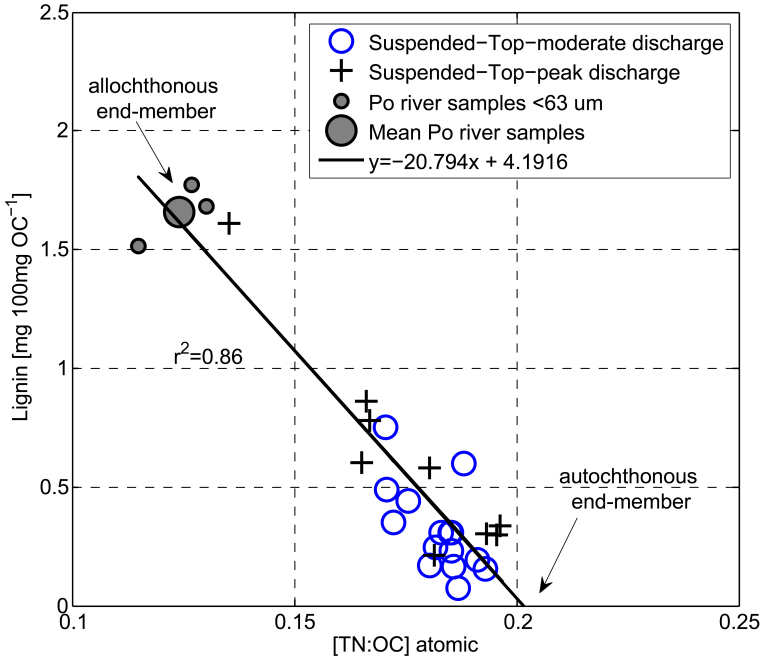

Fig. 11. Plot of TN:OC vs. lignin. Open circles and crosses are surface suspended sediments collected during moderate and peak flood, respectively. Filled circles are fine material (<63 µm) collected in the Po river. Solid line is the regression line.

BGD
7, 7849–7902, 2010

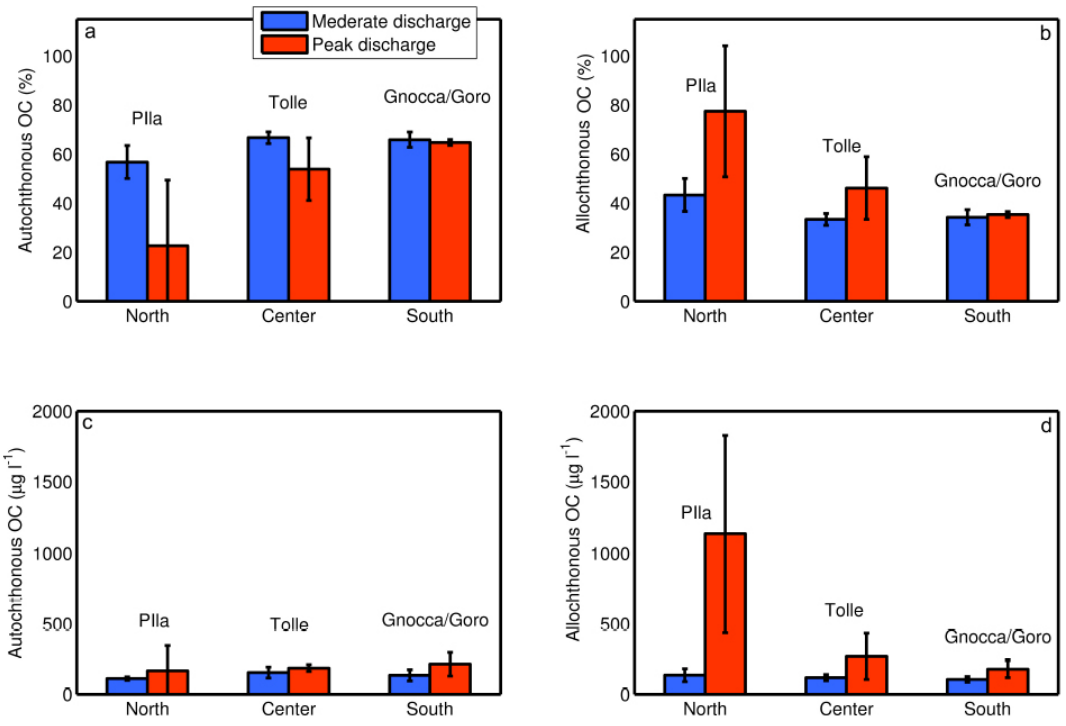

Fig. 12. Results from the end-member mixing model. Surface suspended samples were grouped in three sub-regions according to the latitude: north, center, south. Blu and red are samples collected during moderate and peak discharge, respectively. **(a)** Fraction of autochthonous OC, **(b)** Fraction of allochthonous OC, **(c)** Concentration of autochthonous OC in the surface plume, and **(d)** Concentration of allochthonous OC in the surface plume.

BGD
7, 7849–7902, 2010